

θ_{13} and charged lepton flavor violation in “warped” A_4 models

Avihay Kadosh^a

^a *Centre for Theoretical Physics, University of Groningen, 9747 AG, Netherlands*
a.kadosh@rug.nl

Abstract

We recently proposed a spontaneous A_4 flavor symmetry breaking scheme implemented in a warped extra dimensional setup to explain the observed pattern of quark and lepton masses and mixings. The main features of this choice are the explanation of fermion mass hierarchies by wave function overlaps, the emergence of tribimaximal (TBM) neutrino mixing and zero quark mixing at the leading order and the absence of tree-level gauge mediated flavor violation. Quark mixing and deviations from TBM neutrino mixing are induced by the presence of bulk A_4 flavons, which allow for “cross-brane” interactions and a “cross-talk” between the quark and neutrino sectors.

In this work, we study the constraints associated with the recent measurements of $\theta_{13} \approx 9^\circ$ by RENO and Daya Bay, forcing every model that predicts TBM neutrino mixing to account for the significant deviation of θ_{13} from 0, while keeping the values of θ_{12} and θ_{23} close to their central experimental values. We then proceed to study in detail the RS- A_4 contributions to $\mu \rightarrow e, 3e$, generated at the tree level by virtue of anomalous Z couplings. These couplings arise from gauge and fermionic KK mixing effects after electroweak symmetry breaking. Since the experimental sensitivity for $BR(\mu \rightarrow e, 3e)$ is expected to increase by five orders of magnitude within the next decade, it is shown that the RS- A_4 lepton sector can be significantly constrained. Finally, we show that when “cross-brane” interactions are turned off, the Z couplings are protected against all anomalous contributions and a strong correlation between θ_{13} and the deviation from maximality of θ_{23} is found.

1 Introduction

Recently we have proposed a model [1] based on a bulk A_4 flavor symmetry [2, 3] in warped geometry [4], in an attempt to account for the hierarchical charged fermion masses, the hierarchical mixing pattern in the quark sector and the large mixing angles and mild hierarchy of masses in the neutrino sector. In analogy with a previous RS realizations of A_4 for the lepton sector [5, 6], the three generations of left-handed (LH) quark doublets are unified into a triplet of A_4 ; this assignment forbids tree level FCNCs driven by the exchange of KK gauge bosons, as long as only brane localized effects are considered. The scalar sector of the RS- A_4 model consists of two bulk flavon fields, in addition to a bulk Higgs field. The bulk flavons transform as triplets of A_4 , and allow for a complete "cross-talk" [7] between the $A_4 \rightarrow Z_2$ spontaneous symmetry breaking (SSB) pattern associated with the heavy neutrino sector - with scalar mediator peaked towards the UV brane - and the $A_4 \rightarrow Z_3$ SSB pattern associated with the quark and charged lepton sectors - with scalar mediator peaked towards the IR brane - allowing us to obtain realistic mixing angles in the quark sector and deviations from TBM mixing in the neutrino sector. A bulk custodial symmetry, broken differently at the two branes [8], guarantees the suppression of large contributions to electroweak precision observables [9], such as the Peskin-Takeuchi S, T parameters. However, the mixing between zero modes of the 5D theory and their Kaluza-Klein (KK) excitations - after 4D reduction - may still cause significant new physics (NP) contributions to SM suppressed flavor changing neutral current (FCNC) processes.

In [10] we have performed a thorough study of the RS- A_4 contributions to one loop $\Delta F = 1$ dipole transitions (nEDM, $\epsilon'/\epsilon_K, b \rightarrow s(d)\gamma$) and tree level Higgs mediated FCNC $\Delta F = 2$ transitions ($K^0 - \bar{K}^0$ and $D^0 - \bar{D}^0$ mixing). The main difference between the RS- A_4 setup and an anarchic RS flavor scheme [11] lies in the degeneracy of fermionic LH bulk mass parameters, which implies the universality of LH zero mode profiles and hence forbids gauge mediated FCNC processes at tree level, including the KK gluon exchange contribution to ϵ_K . The latter provides the most stringent constraint on flavor anarchic models, together with the neutron EDM (nEDM) [11, 12]. However, the choice of the common LH bulk mass parameter, c_q^L is strongly constrained by the matching of the top quark mass ($m_t(1.8 \text{ TeV}) \approx 140 \text{ TeV}$) and the perturbativity bound of the 5D top Yukawa coupling, y_t . Most importantly, when considering the tree level corrections to the $Zb\bar{b}$ coupling against the stringent electroweak precision measurements (EWPM) at the Z pole, we showed [1] that for an IR scale, $\Lambda_{IR} \simeq 1.8 \text{ TeV}$ and $m_h \approx 125 \text{ GeV}$, c_q^L is constrained to be larger than 0.34. Assigning $c_q^L = 0.4$ and matching with m_t we obtain $|y_t| < 3$, which easily satisfies the 5D Yukawa perturbativity bound. For $\Lambda_{IR} \simeq 1.8 \text{ TeV}$ the lightest fermionic KK mode is $\tilde{b}^{(1)}$, the "fake" (custodial) $SU(2)_R$ partner of the 5D fermion, whose zero mode is identified with t_R , with $M_{KK}^{\tilde{b}} \simeq 0.95 \text{ TeV}$. The second most significant constraint on the KK mass scale comes from one-loop Higgs mediated dipole operator contributions to the $b \rightarrow s\gamma$ process, $M_{KK}^{b \rightarrow s\gamma} \simeq 2.55 \Lambda_{IR}^{b \rightarrow s\gamma} \gtrsim 1.3 Y \text{ TeV}$, where Y is the overall scale of the dimensionless 5D Yukawa coefficients. The constraints on M_{KK} coming from ϵ'/ϵ_K (nEDM) were shown to be weaker by at least factor of 2(6) (See [10]).

In this paper we focus on the charged lepton and neutrino sectors of the RS- A_4 setup. We start by performing a systematic study of the RS- A_4 predictions for the neutrino mixing angles in light of the recent measurements of $\theta_{13} \approx 9^\circ$ by the RENO [13], Daya Bay [14] and DOUBLECHOOZ [15] experiments, supporting previous indications in T2K [16] and MINOS [17]. It is shown that significant deviations from TBM neutrino mixing are generated by both “cross talk” interactions in the charged lepton sector and higher order corrections to the heavy Majorana and (light) Dirac mass matrices. The model predictions are then compared with the results of the most recent global fits [18, 19]. Subsequently, we inspect the RS- A_4 contributions to the charged lepton flavor violating processes $\mu \rightarrow 3e$ and $\mu \rightarrow e$ conversion. We show that the dominant contributions come from tree-level Z boson exchange diagrams, where the flavor violating Z boson couplings are induced by gauge and fermion KK mixing effects. We then compare our predictions with the existing upper bounds [20, 21] and those expected to come from a series of experiments, currently under construction in J-PARC [22–24], Osaka (RNCP) [25], Fermilab [26, 27] and PSI [28] within the next decade.

The paper is organized as follows. In Sec. 2 we summarize the most relevant features of the RS- A_4 setup needed for the analysis of the following sections. In Sec. 3 we study the modifications of the PMNS matrix induced by higher order effects in both the neutrino and the charged lepton sectors and perform a numerical scan to test our predictions against the experimental bounds. In Sec. 3.1 we specialize to the brane localized RS- A_4 setup. In Sec. 4 we study the effect of gauge boson and KK fermion mixing on Z couplings and obtain analytical estimations of the $Z\mu e$ coupling relevant for the $\mu \rightarrow e, 3e$ processes. In Sec. 4.4 we obtain the exact results by a numerical diagonalization of the zero+KK mass matrices and perform a scan over the parameter space of the RS- A_4 setup including/excluding cross-brane effects. It is shown that the brane localized version of RS- A_4 stays protected from KK mixing contributions to off diagonal Z couplings. We conclude in Sec. 5.

2 The RS- A_4 model

The RS- A_4 setup [1] is illustrated in Fig. 1. The bulk geometry is that of a slice of AdS_5 compactified on an orbifold S_1/Z_2 [4] and is described by the metric on the bottom of Fig. 1. All 5D fermionic fields propagate in the bulk and transform under the following representations of $(SU(3)_c \times SU(2)_L \times SU(2)_R \times U(1)_{B-L}) \times A_4 \times Z_2$ [1]:

$$\begin{aligned}
e_R \oplus e'_R \oplus e''_R &\sim (1, 1, 2, -1) (\underline{\mathbf{1}} \oplus \underline{\mathbf{1}}' \oplus \underline{\mathbf{1}}'') (+), & \ell_L &\sim (1, 2, 1, -1) (\underline{\mathbf{3}}) (-), \\
u_R \oplus u'_R \oplus u''_R &\sim (3, 1, 2, \frac{1}{3}) (\underline{\mathbf{1}} \oplus \underline{\mathbf{1}}' \oplus \underline{\mathbf{1}}'') (+), & \nu_R &\sim (1, 1, 2, 0) (\underline{\mathbf{3}}) (-), \\
d_R \oplus d'_R \oplus d''_R &\sim (3, 1, 2, \frac{1}{3}) (\underline{\mathbf{1}} \oplus \underline{\mathbf{1}}' \oplus \underline{\mathbf{1}}'') (+), & Q_L &\sim (3, 2, 1, \frac{1}{3}) (\underline{\mathbf{3}}) (-).
\end{aligned} \tag{1}$$

The SM fermions, including right handed (RH) neutrinos, are identified with the zero modes of the 5D fermions above. The zero (and KK) mode profiles are determined by the bulk mass

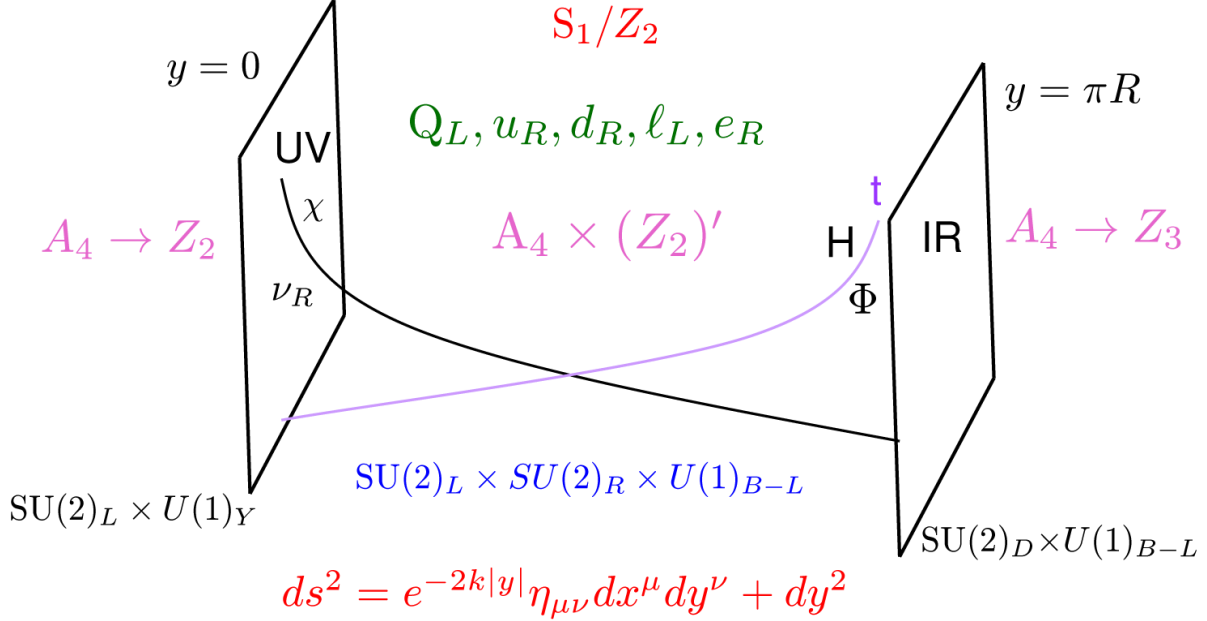


Figure 1: A pictorial description of the RS- A_4 setup. The bulk geometry is described by the metric at the bottom and $k \simeq M_{Pl}$ is the AdS_5 curvature scale. All fields propagate in the bulk and the UV(IR) peaked nature of the heavy RH neutrinos, the Higgs field, the t quark and the A_4 flavons, Φ and χ , is emphasized. The SSB patterns of the bulk symmetries on the UV and IR branes are specified on the side (for A_4) and on the bottom (for $SU(2)_L \times SU(2)_R \times U(1)_{B-L}$) of each brane.

of the corresponding 5D fermion, denoted by $c_{q_L, u_i, d_i, e_i} k$ and boundary conditions (BC) [10]. The scalar sector contains the IR peaked Higgs field and the UV and IR peaked flavons, χ and Φ , respectively. They transform as:

$$\Phi \sim (1, 1, 1, 0) (\underline{\mathbf{3}}) (-), \quad \chi \sim (1, 1, 1, 0) (\underline{\mathbf{3}}) (+), \quad H (1, 2, 2, 0) (\underline{\mathbf{1}}) (+). \quad (2)$$

The SM Higgs field is identified with the first KK mode of H . All fermionic zero modes acquire masses through Yukawa interactions with the Higgs field and the A_4 flavons after SSB. The 5D $(SU(3)_c \times SU(2)_L \times SU(2)_R \times U(1)_{B-L}) \times A_4 \times Z_2$ invariant Yukawa Lagrangian will consist of only UV/IR peaked interactions at the leading order (LO), while at the next to leading order (NLO) it will also give rise to “cross-talk” and “cross-brane” effects [1]. The LO interactions in the neutrino sector are shown in [1] using the see-saw I mechanism, to induce a tribimaximal (TBM) [29] pattern for neutrino mixing. Below we are going to show that “cross brane” and “cross talk” interactions, induce deviations from TBM, such that the model predictions for $\theta_{12,23,13}$ are in good agreement with the current experimental bounds [18,19]. Starting from the quark and charged lepton sectors, the most relevant terms of the 5D Yukawa Lagrangian are of the following form:

$$\mathcal{L}_{5D}^{Yuk.} \supset \underbrace{\frac{y_{u_i, d_i, e_i}}{k^2} (\bar{Q}_L, \bar{\ell}_L) \Phi H(u_R^{(i, \prime\prime)}, d_R^{(i, \prime\prime)}, e_R^{(i, \prime\prime)})}_{\mathcal{L}_{LO}} + \underbrace{\frac{(\tilde{x}_i^{u, d, \ell}, \tilde{y}_i^{u, d, \ell})}{k^{7/2}} (\bar{Q}_L, \bar{\ell}_L) \Phi \chi H(u_R^{(i, \prime\prime)}, d_R^{(i, \prime\prime)}, e_R^{(i, \prime\prime)})}_{\mathcal{L}_{NLO}}. \quad (3)$$

Notice that the LO interactions are peaked towards the IR brane while the NLO interactions mediate between the two branes due to the presence of both Φ and χ .

The VEV and physical profiles for the bulk scalars are obtained by solving the corresponding equations of motion with a UV/IR localized quartic potential term and an IR/UV localized mass term [30]. In this way one can obtain either UV or IR peaked and also flat profiles depending on the bulk mass and the choice of boundary conditions. The resulting VEV profiles of the RS- A_4 scalar sector are:

$$v_{H(\Phi)}^{5D} = H_0(\phi_0) e^{(2+\beta_{H(\Phi)})k(|y|-\pi R)} \quad v_\chi^{5D} = \chi_0 e^{(2-\beta_\chi)k|y|} (1 - e^{(2\beta_\chi)k(|y|-\pi R)}), \quad (4)$$

where $\beta_{H, \Phi, \chi} = \sqrt{4 + \mu_{H, \Phi, \chi}^2}$ and $\mu_{H, \Phi, \chi}$ is the bulk mass of the corresponding scalar in units of k , the cutoff of the 5D theory. The following vacua for the Higgs and the A_4 flavons Φ and χ ,

$$\langle \Phi \rangle = (v_\phi, v_\phi, v_\phi) \quad \langle \chi \rangle = (0, v_\chi, 0) \quad \langle H \rangle = v_H \begin{pmatrix} 1 & 0 \\ 0 & 1 \end{pmatrix}, \quad (5)$$

provide at LO zero quark mixing and TBM neutrino mixing [2, 7]. The stability of the above vacuum alignment is discussed in [1]. The VEV of Φ induces an $A_4 \rightarrow Z_3$ SSB pattern, which in turn induces no quark mixing and is peaked towards the IR brane. Similarly, the VEV of χ induces an $A_4 \rightarrow Z_2$ SSB pattern peaked towards the UV brane. Subsequently, NLO interactions, including both Φ and χ , break A_4 completely and induce quark mixing and deviations from TBM. The Higgs VEV is in charge of the SSB pattern $SU(2)_L \times SU(2)_R \rightarrow SU(2)_D$, which is peaked towards the IR brane. The (gauge) SSB pattern on the UV brane is driven by orbifold BC and a Planckian UV localized VEV, which is effectively decoupled from the model [8].

To summarize the implications of the NLO interactions in the quark and charged lepton sectors, we provide the structure of the LO+NLO mass matrices in the ZMA [1]:

$$\frac{1}{v} (M + \Delta M)_{u, d, \ell}^{AD} = \underbrace{\begin{pmatrix} y_{u, d, e}^{AD} & y_{c, s, \mu}^{AD} & y_{t, b, \tau}^{AD} \\ y_{u, d, e}^{AD} & \omega y_{c, s, \mu}^{AD} & \omega^2 y_{t, b, \tau}^{AD} \\ y_{u, d, e}^{AD} & \omega^2 y_{c, s, \mu}^{AD} & \omega y_{t, b, \tau}^{AD} \end{pmatrix}}_{\sqrt{3}U(\omega) \text{diag}(y_{u_i, d_i, e_i}^{AD})} + \begin{pmatrix} f_\chi^{u, d, e} x_1^{u, d, \ell} & f_\chi^{c, s, \mu} x_2^{u, d, \ell} & f_\chi^{t, b, \tau} x_3^{u, d, \ell} \\ 0 & 0 & 0 \\ f_\chi^{u, d, e} y_1^{u, d, \ell} & f_\chi^{c, s, \mu} y_2^{u, d, \ell} & f_\chi^{t, b, \tau} y_3^{u, d, \ell} \end{pmatrix}, \quad (6)$$

where $\omega = e^{2\pi i/3}$, $v = 174 \text{ GeV}$ is the 4D Higgs VEV, $y_{u, c, t, d, s, b, e, \mu, \tau}^{AD}$ are the effective 4D LO Yukawa couplings, $(x_i^\ell, y_i^\ell) \equiv (\tilde{x}_i^\ell, \tilde{y}_i^\ell) y_{u_i, d_i, e_i}^{AD} / y_{u_i, d_i, e_i}$ and $y_{u_i, d_i, e_i} (\tilde{x}_i^{u, d, \ell}, \tilde{y}_i^{u, d, \ell})$ are the 5D LO (NLO) Yukawa couplings. The function $f_\chi^{u_i, d_i, e_i} \simeq 2\beta_\chi C_\chi / (12 - c_{qL, \ell L} - c_{u_i, d_i, e_i}) \simeq 0.05$ accounts for the suppression of the NLO Yukawa interactions and $C_\chi \equiv \chi_0 / M_{Pl}^{3/2} \simeq 0.155$.

Finally, the unitary matrix, $U(\omega)$ is the LO left diagonalization matrix in both the up and down sectors, $(V_L^{u,d,\ell})_{LO}$, which is independent of the LO Yukawa couplings, while $(V_R^{u,d,\ell})_{LO} = \mathbb{1}$ (see [1]). Using standard perturbative techniques on the matrix in Eq. (6) we obtained $(V_{L,R}^{u,d,\ell})_{NLO}$ [1, 10] at $\mathcal{O}(f_\chi^{u_i,d_i,e_i}(\tilde{x}_i^{u,d,\ell}, \tilde{y}_i^{u,d,\ell}))$. The left-handed diagonalization matrix is given by

$$V_L^{q,\ell} = U(\omega) \begin{pmatrix} 1 & f_\chi^{c,s,\mu}(\tilde{x}_2^{q,\ell} + \tilde{y}_2^{q,\ell}) & f_\chi^{t,b,\tau}(\tilde{x}_3^{q,\ell} + \tilde{y}_3^{q,\ell}) \\ -f_\chi^{c,s,\mu}[(\tilde{x}_2^{q,\ell})^* + (\tilde{y}_2^{q,\ell})^*] & 1 & f_\chi^{t,b,\tau}(\tilde{x}_3^{q,\ell} + \omega\tilde{y}_3^{q,\ell}) \\ -f_\chi^{t,b,\tau}[(\tilde{x}_3^{q,\ell})^* + (\tilde{y}_3^{q,\ell})^*] & -f_\chi^{t,b,\tau}[(\tilde{x}_3^{q,\ell})^* + \omega^2(\tilde{y}_3^{q,\ell})^*] & 1 \end{pmatrix}, \quad (7)$$

where $q = u, d$.

Similarly, the right diagonalization matrices in the quark and charged lepton sectors, to first order in $f_\chi^{u_i,d_i,e_i}(\tilde{x}_i^{u,d,\ell}, \tilde{y}_i^{u,d,\ell})$ are given by

$$V_R^{q,\ell} = \begin{pmatrix} 1 & \Delta_1^{q,\ell} & \Delta_2^{q,\ell} \\ -(\Delta_1^{q,\ell})^* & 1 & \Delta_3^{q,\ell} \\ -(\Delta_2^{q,\ell})^* & -(\Delta_3^{q,\ell})^* & 1 \end{pmatrix}, \quad (8)$$

where $q = u, d$ and the $\Delta_i^{q,\ell}$ are given by:

$$\Delta_1^{q,\ell} = \frac{m_{u,d,e}}{m_{c,s,\mu}} \left[f_\chi^{u,d,e} \left((\tilde{x}_1^{q,\ell})^* + \omega^2(\tilde{y}_1^{q,\ell})^* \right) + f_\chi^{c,s,\mu} \left(\tilde{x}_2^{q,\ell} + \tilde{y}_2^{q,\ell} \right) \right], \quad (9)$$

$$\Delta_2^{q,\ell} = \frac{m_{u,d,e}}{m_{t,b,\tau}} \left[f_\chi^{u,d,e} \left((\tilde{x}_1^{q,\ell})^* + \omega(\tilde{y}_1^{q,\ell})^* \right) + f_\chi^{t,b,\tau} \left(\tilde{x}_3^{q,\ell} + \tilde{y}_3^{q,\ell} \right) \right], \quad (10)$$

$$\Delta_3^{q,\ell} = \frac{m_{c,s,\mu}}{m_{t,b,\tau}} \left[f_\chi^{c,s,\mu} \left((\tilde{x}_2^{q,\ell})^* + \omega(\tilde{y}_2^{q,\ell})^* \right) + f_\chi^{t,b,\tau} \left(\tilde{x}_3^{q,\ell} + \omega\tilde{y}_3^{q,\ell} \right) \right]. \quad (11)$$

The suppression by quark mass ratios of the off-diagonal elements in $V_R^{u,d}$, stemming from the degeneracy of LH bulk masses, turned out to play an important role in relaxing the flavor violation bounds on the KK mass scale, as compared to flavor anarchic frameworks [10].

3 The neutrino sector – Higher order corrections to the PMNS matrix and θ_{13}

The global fits based on the recent measurements of $\nu_\mu \rightarrow \nu_e$ appearance in the RENO, Daya Bay, T2K, MINOS and other experiments, allow one to obtain a significance of 10σ for $\theta_{13} > 0$, with best fit points at around $\theta_{13} \simeq 0.15$, depending on the precise treatment of reactor fluxes [18, 19]. We wish the RS- A_4 higher order corrections to the PMNS matrix to be such that the new fits are still “accessible” by a significant portion of the model parameter space.

In the RS- A_4 model deviations from TBM neutrino mixing are generated by higher order effects on the UV/IR branes and by “cross-talk” and “cross-brane” effects. In [1] we studied in detail the textures induced by the three types of higher order corrections. Here we quote the dominant corrections to the Dirac and Majorana mass matrices and the resulting modification of V_L^ν the left diagonalization matrix of the effective (LL) neutrino Majorana mass matrix.

Starting from the Dirac mass terms we have:

$$\mathcal{L}_\nu^D \subset k^{-1/2} y_\nu \bar{\ell}_L H \nu_R + k^{-2} y_\chi^D \bar{\ell}_L H \chi \nu_R + k^{-7/2} y_D^{\Phi^2} \bar{\ell}_L H \Phi^2 \nu_R, \quad (12)$$

where y_ν , y_D^χ and $y_D^{\Phi^2}$ are dimensionless 5D Yukawa couplings. The 4D effective mass matrix is obtained by integrating over y the profiles of the fields/VEV’s in each of the above operators and acquires the following form [1]:

$$\hat{M}_\nu^D = m_\nu^D \begin{pmatrix} 1 + \epsilon_1 & \epsilon_2 & \epsilon_3 + \epsilon_\chi \\ \epsilon_3 & 1 + \epsilon_1 & \epsilon_2 \\ \epsilon_2 + \epsilon_\chi & \epsilon_3 & 1 + \epsilon_1 \end{pmatrix}, \quad (13)$$

where the m_ν^D , ϵ_χ and $\epsilon_{1,2,3}$ entries come from the first, second and third terms of Eq. (12), respectively. Notice that the smallness of $\epsilon_{\chi,1,2,3}$ compared to m_ν^D comes not only from the (mild) suppression of the flavon VEV’s with respect to the 5D scale $k \sim \mathcal{O}(M_{Pl})$ but also from the associated overlap correction factors [1, 10].

Turning to the Majorana mass terms we have:

$$\mathcal{L}_\nu^M \subset M \bar{\nu}_R^c \nu_R + k^{-1/2} y_{\chi\chi} \bar{\nu}_R^c \nu_R + k^{-2} y_{\chi^2} \chi^2 \bar{\nu}_R^c \nu_R, \quad (14)$$

The resulting 4D (heavy) Majorana mass matrix acquires the following form:

$$\hat{M}_\nu^M = \tilde{M} \begin{pmatrix} 1 + \epsilon_4 & 0 & M_\chi / \tilde{M} \\ 0 & 1 + \epsilon_5 & 0 \\ M_\chi / \tilde{M} & 0 & 1 + \epsilon_4^* \end{pmatrix}, \quad (15)$$

where \tilde{M} , M_χ and $\epsilon_{4,5}$ come from the first, second and third terms of Eq. (14). The smallness of $\epsilon_{4,5}$ comes mainly from the suppression associated with the flavon VEV’s, since the effect of overlap corrections is milder for UV peaked operators [1].

The effective (light) Majorana mass matrix is now obtained using the see-saw mechanism, $\hat{M}_\nu^{eff} = -(\hat{M}_\nu^D)^T (\hat{M}_\nu^M)^{-1} \hat{M}_\nu^D$. If we turn off $\epsilon_{1-5,\chi}$ we obtain the LO results of [1], for which the mass spectrum is given by

$$(\hat{M}_{eff}^\nu)_{diag.} = (V_L^\nu)^T \hat{M}_{eff}^\nu V_L^\nu = -\frac{(m_\nu^D)^2}{\tilde{M}} \text{diag} \left[\frac{1}{1+q}, 1, \frac{1}{1-q} \right] \quad (16)$$

where $q \equiv M_\chi / \tilde{M}$. Notice that the overall neutrino mass scale is set by the ratio $(m_\nu^D)^2 / \tilde{M}$, while the type of hierarchy and its extent are determined by q . Using $\Delta m_{atm}^2 \simeq 2.43 \cdot 10^{-3} \text{eV}^2$

and $\Delta m_{sol}^2 \simeq 7.6 \cdot 10^{-5} \text{eV}^2$ from [18], we are able to obtain a cubic equation for q with solutions $q \simeq [-2.02, -1.98, 0.79, 1.19]$, where the first (last) two solutions correspond to inverted (normal) mass hierarchy [1]. The LO diagonalization matrix V_L^ν is given by:

$$V_L^\nu = \begin{pmatrix} 1/\sqrt{2} & 0 & -1/\sqrt{2} \\ 0 & 1 & 0 \\ 1/\sqrt{2} & 0 & 1/\sqrt{2} \end{pmatrix}. \quad (17)$$

We now proceed to obtain the corrections to V_L^ν considering the higher order effects encoded in Eqs. (13) and (15). Since numerically $\epsilon_{1-5,\chi} \sim 0.05$, we can perform (analytically) the perturbative diagonalization of $(\hat{M}_\nu^{eff})_{NLO}$ to leading order in each of the ϵ 's. The resulting $(V_L^\nu)_{NLO} \equiv \tilde{V}_L^\nu$ is given by:

$$\tilde{V}_L^\nu = \begin{pmatrix} \frac{1}{\sqrt{2}} + \frac{\epsilon_2^* - \epsilon_3^*}{2\sqrt{2}} - i \frac{q^2 - 1}{2\sqrt{2}q} \text{Im}(\epsilon_4) & \frac{\epsilon_2 + \epsilon_3}{q} + i \text{Im}(\epsilon_2) + \text{Re}(\epsilon_3) & -\frac{1}{\sqrt{2}} + \frac{\epsilon_2 - \epsilon_3}{2\sqrt{2}} + i \frac{q^2 - 1}{2\sqrt{2}q} \text{Im}(\epsilon_4) \\ -\frac{2+q}{\sqrt{2}q} (\epsilon_2^* + \epsilon_3^*) & 1 & \frac{\epsilon_3 - \epsilon_2}{\sqrt{2}} \\ \frac{1}{\sqrt{2}} - \frac{\epsilon_2^* - \epsilon_3^*}{2\sqrt{2}} + i \frac{q^2 - 1}{2\sqrt{2}q} \text{Im}(\epsilon_4) & \frac{\epsilon_2 + \epsilon_3}{q} + i \text{Im}(\epsilon_3) + \text{Re}(\epsilon_2) & \frac{1}{\sqrt{2}} + \frac{\epsilon_2 - \epsilon_3}{2\sqrt{2}} + i \frac{q^2 - 1}{2\sqrt{2}q} \text{Im}(\epsilon_4) \end{pmatrix}. \quad (18)$$

Using V_L^ℓ of Eq. (7) and (\tilde{V}_L^ν) of Eq. (18), we obtain the modified PMNS matrix, which includes all dominant higher order effects from the charged lepton and neutrino sectors, $V_{PMNS} \equiv W = (V_L^\ell)^\dagger \tilde{V}_L^\nu$. Notice that all elements of the PMNS matrix will be still independent of the LO Yukawa couplings $(y_{e,\mu,\tau,\nu,\chi,M})$, due to the Form diagonalizability of the LO mass matrices. We avoid writing the resulting PMNS matrix explicitly, due to its complexity. By expanding the basis independent relations

$$\theta_{13} = \arcsin|W_{13}|, \quad \theta_{12} = \arctan(|W_{12}|/|W_{11}|), \quad \theta_{23} = \arcsin(|W_{23}|/|W_{33}|), \quad (19)$$

we are able to obtain approximate analytical expressions for $\theta_{12,13,23}$,

$$\sin \theta_{12} \simeq \frac{1}{\sqrt{3}} \left| 1 + \frac{2+q}{3q} \left(\epsilon_2 + \epsilon_3 + 2\text{Re}(\epsilon_2 + \epsilon_3) \right) - \tilde{f}_\chi^{\mu,\tau} \left(\omega^2(x_2^\ell + y_2^\ell) + \omega(x_3^\ell + y_3^\ell) \right) \right|, \quad (20)$$

$$\sin \theta_{13} \simeq \frac{1}{\sqrt{6}} \left| \tilde{f}_\chi^{\mu,\tau} \left[(x_2^\ell + y_2^\ell)(1 - \omega) + (x_3^\ell + y_3^\ell)(1 - \omega^2) \right] + \frac{i(q^2 - 1)}{q} \text{Im} \epsilon_4 \right|, \quad (21)$$

$$\sin \theta_{23} \simeq \frac{1}{\sqrt{2}} \left| -\omega + i\sqrt{3}(\epsilon_2 - \epsilon_3) + \tilde{f}_\chi^{\mu,\tau} \left(\omega^2 x_3^\ell + \omega x_3^{\ell*} + 2\text{Re}(y_3^\ell) \right) + \frac{i(q^2 - 1)}{\sqrt{3}q} \text{Im} \epsilon_4 \right|. \quad (22)$$

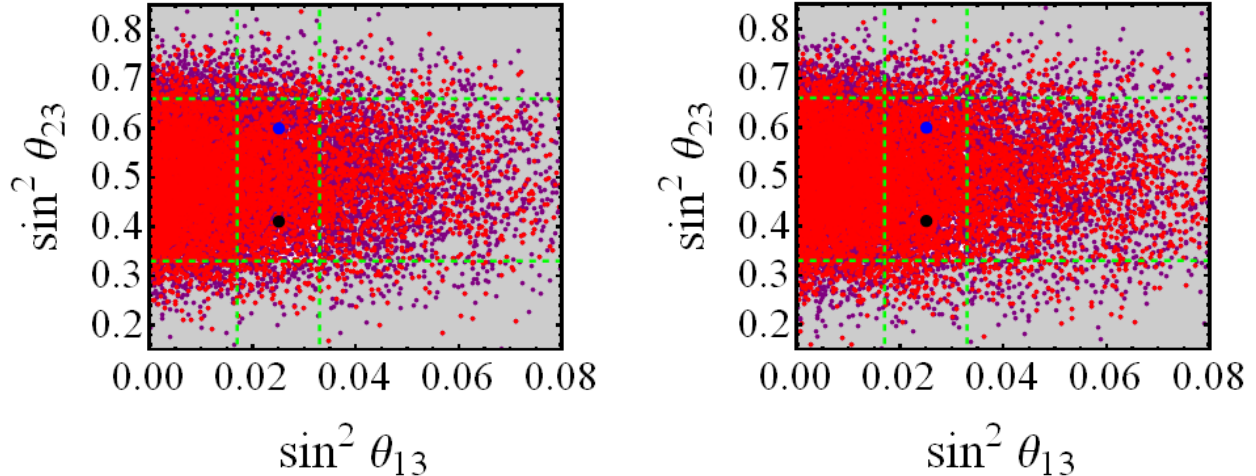


Figure 2: *Model predictions for θ_{23} vs. θ_{13} for normal (left) and inverted (right) mass hierarchy, including all dominant higher order and cross talk effects. The purple points represent the entire sample, while the red points satisfy the 3σ bounds on θ_{12} . The rectangles, confined between the horizontal and vertical dashed green lines, represent the 3σ allowed regions from the global fits of [18, 19].*

We are now ready to perform a systematic study of the RS- A_4 predictions for $\theta_{12,13,23}$. To this end we recall that $\epsilon_{1-5,\chi}$ of Eqs. (13) and (15), implicitly contain the dimensionless Yukawa couplings of their corresponding operator in Eqs. (12) and (14). For this reason $\epsilon_{1-5,\chi}$ will be multiplied by an $\mathcal{O}(1)$ complex Yukawa coupling for the purpose of the numerical scan below. We generate sample of 20000 points, in which all Yukawas ($\tilde{x}_i^\ell, \tilde{y}_i^\ell, y_{e_i}$) are complex numbers with random phases and magnitudes normally distributed around 1 with standard deviation, $\sigma = 0.5$. Using the overlap integrals performed in [1, 10], we get $\epsilon_\chi \simeq 0.07$, $\epsilon_{1,2,3} \simeq 0.04$, $\epsilon_{4,5} \simeq 0.09$ and $\tilde{f}_\chi^{e,\mu,\tau} \equiv \sqrt{3}f_\chi^{e,\mu,\tau} \simeq 0.08$. By Substituting $\epsilon_{1-5,\chi}$ in Eq. (19), we study the correlations between the various neutrino mixing angles. The results of the scan are plotted in Figs. 2–4. The rectangle confined between the dashed green lines represent the 3σ allowed regions from the global fits of [18, 19]. The purple points in each plot represent the entire sample, while the red points, depicted on top of the purple ones, satisfy in addition the 3σ constraint from the mixing angle not appearing in the same figure. In other words, the red points in Fig. 2 satisfy the 3σ constraint on θ_{12} and so on. The best fit point(s) are depicted in black (blue) for $(\theta_{23})_{\text{best}}$ values from the first (second) octant, where $\Delta\chi_{\text{black}}^2 < \Delta\chi_{\text{blue}}^2$ in the global fit of [18].

We realize that there are only mild differences between the NH and IH cases, coming from the terms proportional to $(2+q)$ and (q^2-1) in Eqs. (20)–(22). Qualitatively, this means that the deviations from TBM mixing in the IH case are slightly larger for $\theta_{13,23}$ and slightly smaller for θ_{12} , as can be seen in Figs. 2–4. To quantify the viability of the RS- A_4 setup in predicting realistic neutrino mixing angles, we can define a success rate for the NH and IH cases in analogy with [31]. Namely, we ask ourselves what is the percentage of the

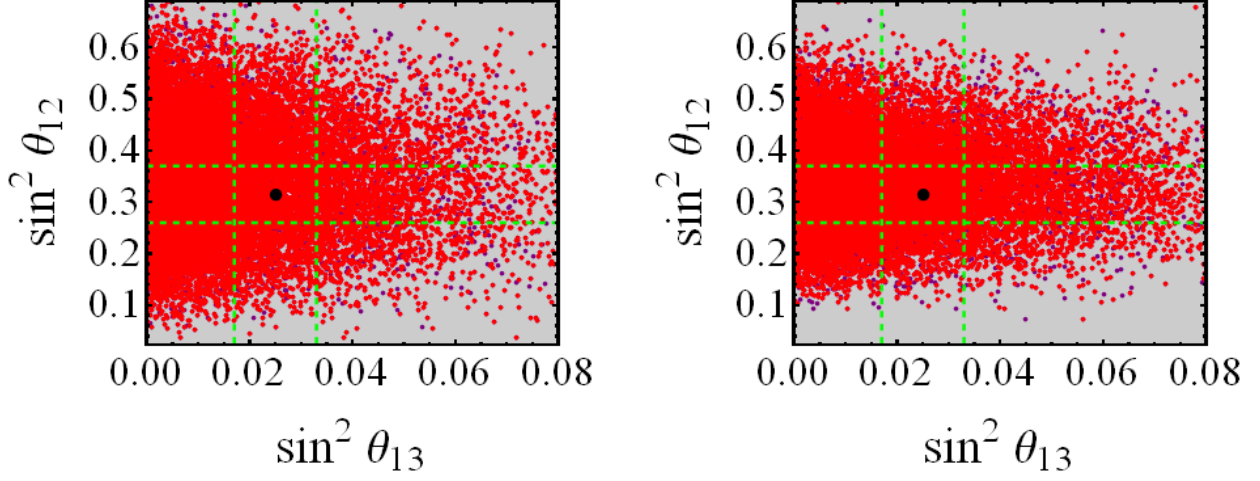


Figure 3: *Model predictions for θ_{12} vs. θ_{13} for normal (left) and inverted (right) mass hierarchy, including all dominant higher order and cross talk effects. The purple points represent the entire sample, while the red points satisfy the 3σ bounds on θ_{23} . The rectangles, confined between the horizontal and vertical dashed green lines, represent the 3σ allowed regions from the global fits of [18, 19].*

points, ξ , satisfying the 3σ constraints for all neutrino mixing angles. We get $\xi_{NH} \simeq 10\%$ and $\xi_{IH} \simeq 12.5\%$, which is slightly better than the results for typical A_4 models in [31]. We avoid analyzing the RS- A_4 predictions for δ_{CP}^ν , due to the lack of sufficient experimental data and its potential sensitivity to higher order effects of $\mathcal{O}(\epsilon_i^2, f_\chi^2)$. The above analysis redemonstrates [32, 33] the viability of models predicting TBM at LO, with corrections coming from higher order effects in both the charged lepton and neutrino sectors and in particular the RS- A_4 setup.

3.1 Simplifications in the brane localized RS- A_4 setup

If we specialize to the brane localized version of the RS- A_4 model [5, 6] the cross talk interactions associated with the $\tilde{x}_{2,3}^\ell$ and $\tilde{y}_{2,3}^\ell$ are absent and the expressions for the mixing angles simplify to the following form:

$$\sin \theta_{13} \simeq \left| \frac{i(q^2 - 1)}{\sqrt{6}q} \text{Im } \epsilon_4 \right|, \quad \sin \theta_{12} \simeq \left| 1 + \frac{2 + q}{3\sqrt{3}q} \left(\epsilon_2 + \epsilon_3 + 2\text{Re}(\epsilon_2 + \epsilon_3) \right) \right| \quad (23)$$

$$\sin \theta_{23} \simeq \left| \frac{1}{2\sqrt{2}} + i \left(-\frac{\sqrt{3}}{2\sqrt{2}} + \sqrt{\frac{3}{2}}(\epsilon_2 - \epsilon_3) + \frac{(q^2 - 1)}{\sqrt{6}q} \text{Im } \epsilon_4 \right) \right|. \quad (24)$$

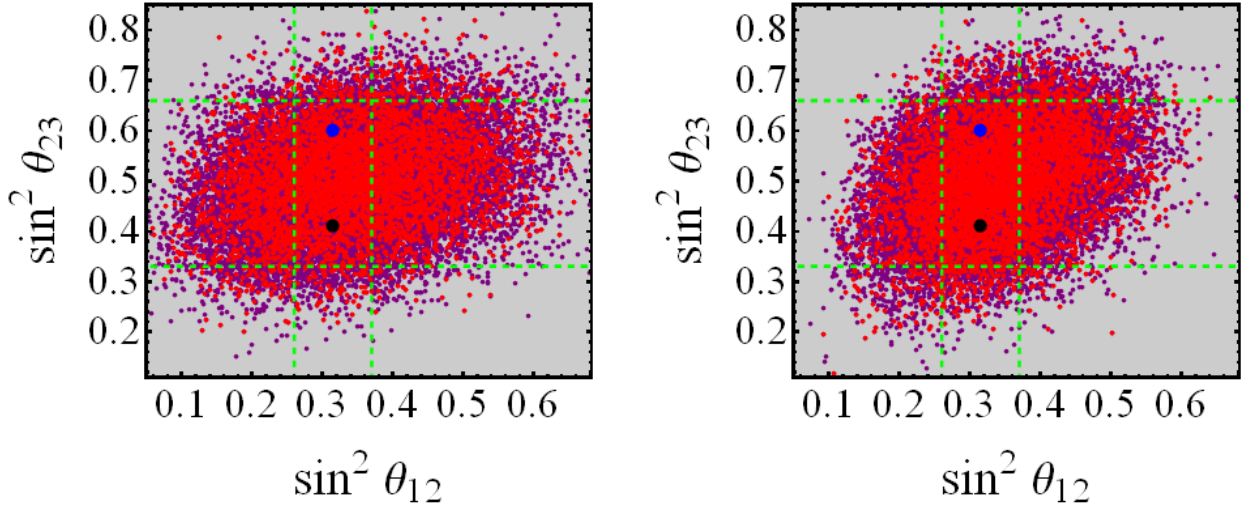


Figure 4: *Model predictions for θ_{23} vs. θ_{12} for normal (left) and inverted (right) mass hierarchy, including all dominant higher order and cross talk effects. The purple points represent the entire sample, while the red points satisfy the 3σ bounds on θ_{13} . The rectangles, confined between the horizontal and vertical dashed green lines, represent the 3σ allowed regions from the global fits of [18, 19].*

We immediately realize that θ_{13} is now governed by q and $\text{Im}(\epsilon_4)$. We take ϵ_4 to be pure imaginary and fix its magnitude to obtain the best fit value $\sin^2(\theta_{13}) \simeq 0.158$ [18, 19]. The fixing of ϵ_4 depends on the type of hierarchy, as determined by $q = M_\chi/\tilde{M}$ (Eq. (16)). For the NH case we get $\text{Im}(\epsilon_4) \simeq 0.5(0.97)$ for $q \simeq 0.79(1.19)$, while for the IH case we have $\text{Im}(\epsilon_4) \simeq 0.6$ for $q = -2.02(-1.98)$. These solutions for $\text{Im}(\epsilon_4)$ implicitly include y_{ϵ_4} , the dimensionless 5D Yukawa coupling of the operator $k^{-2}\chi^2\bar{\nu}_R^c\nu_R$, entering as $\epsilon_4 \equiv k^{-1}y_{\epsilon_4}v_\chi^{UV}$ in the 4D effective theory on the UV brane. For the characteristic value $k^{-1}v_\chi^{UV} \simeq 0.1$ we have $|y_{\epsilon_4}^{NH}| \simeq 5(10.5)$ and $|y_{\epsilon_4}^{IH}| \simeq 6$, all of which satisfy the naive dimensional analysis (NDA) perturbativity bounds from [5] $|y_{\epsilon_4}| < 4\pi$.

Now that we solved for θ_{13} , the values of $\theta_{12,23}$ are controlled by the $\epsilon_{2,3}$ parameters coming from the operator $k^{-2}\bar{\ell}_L H\Phi^2\nu_R$. In general, we want θ_{23} to deviate towards its best fit value in the first octant $\sin^2\theta_{23}^{bestI} \simeq 0.427$ [19] and θ_{12} stay close to its trimaximal value. Observing Eq. (24), we realize that θ_{13} and θ_{23} contain exactly the same correction term proportional to $\text{Im}(\epsilon_4)$, fixed by the value of θ_{13} . Thus, we have a strong correlation between the increase of θ_{13} from zero and the deviation of θ_{23} towards the first (or second) octant. Since $\epsilon_{2,3}$ are of the same strength, we can take them to be pure imaginary and opposite in sign to change θ_{23} to the desired value (θ_{23}^{bestI}) while keeping $\sin\theta_{12} \simeq 1/\sqrt{3}$. Since the latter possibility is highly fine tuned, we find it more instructive to consider the more general case in which $\epsilon_{2,3} \simeq 0.04y_{\epsilon_{2,3}}$, where $y_{\epsilon_{2,3}}$ are complex numbers with random phases and magnitudes normally distributed around 1 with standard deviation of 0.5. In this case, $\theta_{12,23}$ are governed by four parameters, two phases and two Yukawas. We first specify to the case

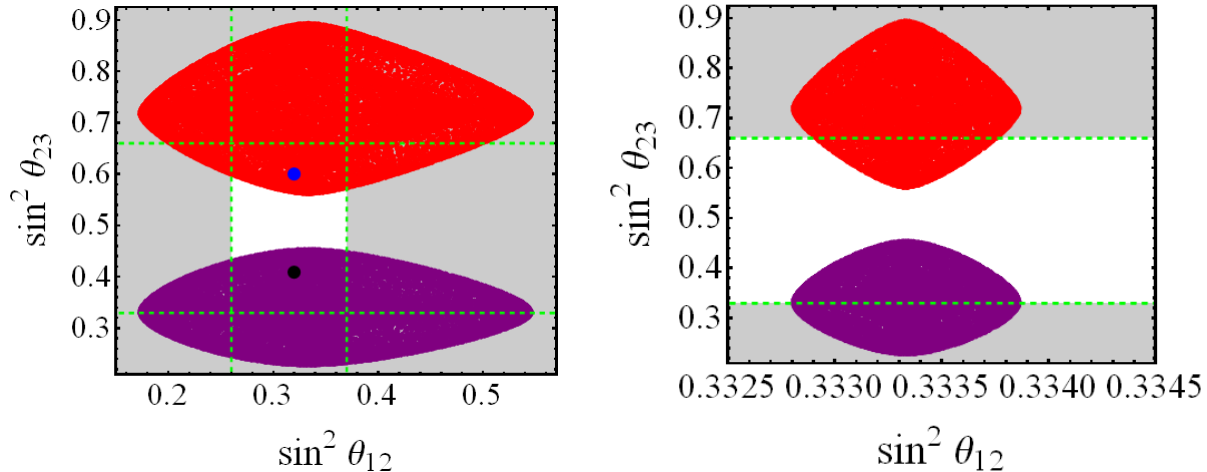


Figure 5: *The brane localized RS- A_4 predictions for θ_{12} vs. θ_{23} for normal (left) and inverted (right) mass hierarchy, including all dominant higher order effects. The best fit value $\sin(\theta_{13}) \simeq 0.158$ fixes $\text{Im}(\epsilon_4)$ up to a sign. The purple (red) points correspond to a positive (negative) value of $\text{Im}(\epsilon_4)$ and we scan over the phases of $\epsilon_{2,3}$ fixing their magnitudes to 0.04 to make the comparison with the “cross-talk” case more transparent. The white rectangles, confined between the horizontal and vertical dashed green lines, represent the 3σ allowed regions from the global fits of [18, 19].*

in which the magnitudes are fixed, where the number of observables equals the number of input parameters, in order to look for a pattern (see also [34]).

We depict the results in Fig. 5. It can be seen that θ_{23} moves strongly to the first (second) octant if $\text{Im}(\epsilon_4)$ is positive (negative) and that the best fit point is rather far from the center of the resulting distributions. It is not sensible to talk about a success rate in such a case due to the assignment imposed by θ_{13} and the simplifying assumptions on $\epsilon_{2,3}$. Relaxing the assumption on the magnitudes of $\epsilon_{2,3}$ have the effect of spoiling the tendency towards the first or second octant, as can be seen by the slight overlap between the “positive” and “negative” cases, as can be seen in Fig. 6.

The analysis of this section shows that the brane localized version of RS- A_4 is more constrained by the experimental neutrino data, due to the fact that the Yukawa coupling associated with ϵ_4 is fixed by θ_{13} to values of order $|y_{\epsilon_4}| \approx 6$ which are still below the perturbativity bound implied by NDA but still render the 5D theory itself less accurate. On the other hand, the small number of parameters ($\epsilon_{2,3,4}$) implies significant simplifications and an interesting correlation between the value of θ_{13} and the (bi-directional) deviations from maximality of θ_{23} . This feature is attributed to the A_4 assignments and vacuum alignment. Finally, the corrections to θ_{12} in the IH case are extremely small due to the absence of ϵ_4 and the $(2 + q)/q$ term in Eq. (20).

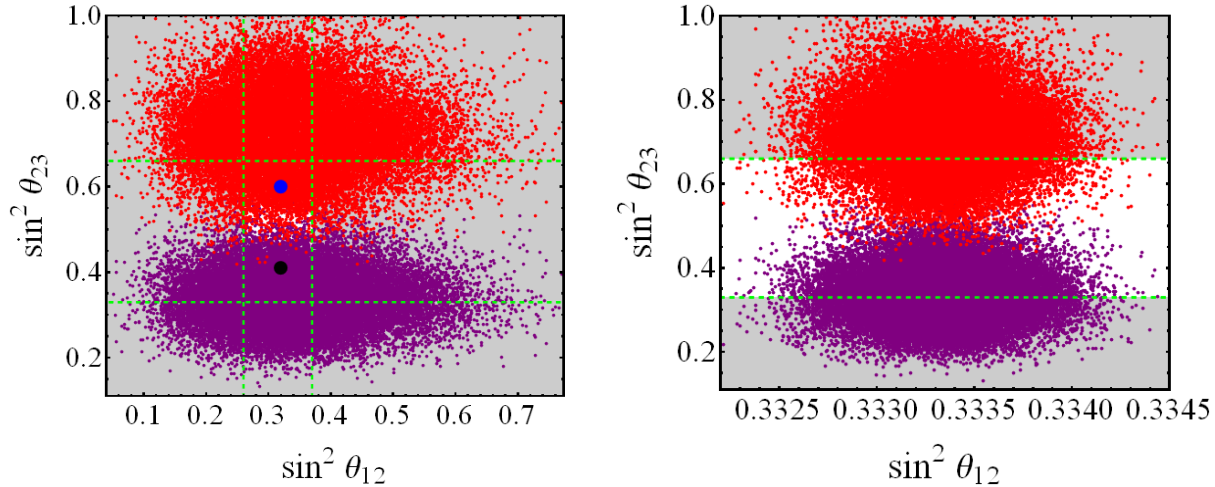


Figure 6: *The brane localized RS- A_4 predictions for θ_{12} vs. θ_{23} for normal (left) and inverted (right) mass hierarchy, scanning over the phases and magnitudes of $\epsilon_{2,3}$. The best fit value $\sin(\theta_{13}) \simeq 0.158$ fixes $\text{Im}(\epsilon_4)$ up to a sign. The purple (red) points correspond to positive (negative) values of $\text{Im}(\epsilon_4)$. The white rectangles, confined between the horizontal and vertical dashed green lines, represent the 3σ allowed regions from the global fit of [18, 19].*

4 The charged lepton sector- Anomalous Z couplings and cLFV

Charged lepton flavor violating processes like $\mu \rightarrow 3e$ and $\mu \rightarrow e$ conversion in the presence of a nucleus are the main focus of a series of experiments, planned to be performed in J-PARC [22–24], Osaka (RNCP) [25], Fermilab [26, 27] and PSI [28], within the next decade and increase the accuracy for these searches by roughly five orders of magnitude. The current upper bounds were set by the SINDRUM ($\mu \rightarrow 3e$) [20] and SINDRUM II ($\mu \rightarrow e$ in Tl_{22}^{48}) [21] experiments.

As stated in the introduction the main source of charged lepton flavor violation (cLFV) in RS- A_4 are anomalous Z couplings, induced by gauge and fermionic KK mixing, generating Tree level Z exchange contributions to $\mu \rightarrow e, 3e, B_s \rightarrow \mu^+ \mu^-$ and other processes. The effect of EWSB on the mixing of the Z boson with its KK partners and those of the (custodial) Z' , can be studied directly in the zero mode approximation (ZMA), by solving the Z equations of motion in the vicinity of an IR boundary term which induces the SSB pattern $SU(2)_L \times SU(2)_R \rightarrow SU(2)_D$ (e.g. [35]). On the other hand, the effect of KK fermion mixing has to be studied by considering the full KK mass matrices [36].

4.1 The impact of gauge boson mixing on Z couplings

The effect of EWSB on gauge bosons mixing translates via the EOM to a distortion of the Z wave function near the IR brane. The advantage in using this procedure is that all gauge

bosons and their KK partners are automatically given in the physical basis. The canonically normalized physical Z boson wave function (profile) is then given by [35]

$$f_Z^{(0)}(y) \simeq \frac{1}{\sqrt{\pi R}} \left[1 + \frac{M_Z^2 e^{2ky}}{4k^2} \left(1 - 2ky \right) \right]. \quad (25)$$

The modified Z wave function will induce small deviations in the Z coupling matrices $A_{L,R}(Z)$, due to the different overlaps of the zero and KK modes profiles with $f_Z^{(0)}(y)$. Schematically the overlap integrals associated with the Z couplings are written as:

$$\begin{aligned} \frac{(g_{L,R}^Z)}{\sqrt{\pi R}} &= (g_{L,R}^Z)_{SM} R_{nm}^Z \\ &= (g_{L,R}^Z)_{SM} \int dy f_Z^{(0)}(y) \hat{\chi}_{L,R}^{(0,1,1^{--},1^{++},1^{+-} \dots)}(c_{\ell,(e,\mu,\tau)}, y) \hat{\chi}_{L,R}^{(0,1,1^{--},1^{++},1^{+-} \dots)}(c_{\ell,(e,\mu,\tau)}, y), \end{aligned} \quad (26)$$

where $(g_{L,R}^Z)_{SM} = (T_L^3)_{\ell,e,\mu,\tau} - Q_{em}^2 \sin^2 \theta_W$ and $\hat{\chi}_{L,R}^{(m)}(c_{\ell,(e,\mu,\tau)}, y)$ are the canonically normalized wave functions for the zero mode fermions and their KK partners (denoted by m and n).

Before EWSB the Z profile is flat and as a consequence the overlap integrals R_{nm}^Z reduce to an integral over the n^{th} and m^{th} KK modes, satisfying $R_{nm}^Z (f_Z^{(0)} = 1/\sqrt{\pi R}) = \delta_{nm}$ by virtue of the orthonormality of the wave functions and implying $[A_{L,R}(Z)] \propto \mathbb{1}^1$. When EWSB takes place, $f_Z^{(0)}$ is given by Eq. (25) and the coupling matrices, $[A_{L,R}(Z)]$ are no longer proportional to the identity. As a result, once the Z coupling matrices will be rotated to the physical basis of the zero+KK fermions, new off diagonal entries will be generated in $A_{L,R}(Z)$, corresponding to flavor and KK number (and BC type) violating Z couplings.

We first focus on the gauge boson contribution to flavor violating Z couplings in the ZMA, since in this case we are able to obtain simple analytical expressions using the left and right diagonalization matrices of Eqs. (7) and (8)–(11). We start by performing the integral in Eq. (26) for the zero modes of ℓ_L and $e_R^{(\prime,\prime)}$ (Eq. (1), which are identified with the charged lepton sector of the SM. Using

$$\hat{\chi}_{L,R}^{(0)}(c, y) = \sqrt{\frac{k(1-2c)}{e^{k\pi R(1-2c)} - 1}} e^{(1/2-c)k|y|}, \quad \hat{\chi}_{L,R}^{(0)}(c, y = \pi R) \equiv \sqrt{2k} F(c), \quad (27)$$

the resulting deviations in the diagonal entries of the Z coupling matrix are given by:

$$g^{Zff} = \sqrt{\pi R} (g_{L,R}^Z)_{SM} R_{00}^Z \simeq (g_{L,R}^Z)_{SM} \left[1 - \frac{M_Z^2 F^2(c)}{\Lambda_{IR}^2 (3-2c)} \left(k\pi R - \frac{5-2c}{2(3-2c)} \right) \right], \quad (28)$$

where $f = \ell, e, \mu, \tau$ and $c = c_{\ell,e,\mu,\tau}$. The physical couplings are obtained by rotating the Z coupling matrices for the zero modes, $[A_{L,R}(Z)]_{00}^G$ to the mass eigenbasis:

$$\left([A_L(Z)]_{00}^G \right)^{mass} = (V_L^\ell)^\dagger [A_L(Z)]_{00}^G V_L^\ell \equiv \sqrt{\pi R} (g_L^Z)_{SM} (V_L^\ell)^\dagger (R_{00}^Z(c_\ell) \cdot \mathbb{1}) V_L^\ell, \quad (29)$$

$$\left([A_R(Z)]_{00}^G \right)^{mass} = (V_R^\ell)^\dagger [A_R(Z)]_{00}^G V_R^\ell \equiv \sqrt{\pi R} (g_R^Z)_{SM} (V_R^\ell)^\dagger \text{diag}[R_{00}^Z(c_{e,\mu,\tau})] V_R^\ell. \quad (30)$$

¹At this stage we ignore the presence of opposite chirality (--) KK fermions and (+-, -+) ‘‘custodians’’, which will be thoroughly discussed in the next section.

Since $[A_L(Z)]_{00}^G \propto \mathbb{1}$, no LH flavor violating Z couplings will be generated through gauge boson mixing after EWSB and in particular $\delta(g_L^{\mu e})_{\text{gauge}} = 0$. On the other hand, the non degeneracy of RH bulk masses imply $[A_R(Z)]_{00}^G \not\propto \mathbb{1}$ and hence $(\delta g_R^{\mu e})_{\text{gauge}} \neq 0$. By using Eqs. (8)–(9) and (28)–(30) we are able to estimate the strength of this effect

$$\delta g_R^{\mu e} \equiv (g_R^{Z\mu e})_{RS-A_4} - \underbrace{(g_R^{Z\mu e})_{SM}}_{\equiv 0} = \left[(V_R^\ell)^\dagger [A_R(Z)]_{00}^G V_R^\ell \right]_{12,21} \simeq \Delta_1^\ell \left(\delta g_R^{Z\mu\mu} - \delta g_R^{Zee} \right), \quad (31)$$

where $\delta g_R^{Z\mu\mu, Zee}$ are defined in an analogous way and extracted directly from Eq. (28). Since $F(c_e)/F(c_\mu) \approx m_e/m_\mu$, the dominant contribution to $(\delta g_R^{\mu e})_{\text{gauge}}$ will come from $\delta g_R^{Z\mu\mu}$. We realize that $(\delta g_R^{\mu e})_{\text{gauge}}$ is suppressed by both $F^2(c_\mu)M_Z^2/\Lambda_{IR}^2$, and $f_\chi^\mu(m_e/m_\mu)$. For the characteristic values, $\Lambda_{IR} \simeq 1.5 \text{ TeV}$, $c_\ell \simeq 0.51$ and $c_\mu \approx 0.63$, we have $\delta(g_R^{\mu e})_{\text{gauge}} \approx 5 \times 10^{-11}$.

4.2 The impact of KK fermion mixing on Z couplings

To account for KK mixing effects, we write the LO KK mass matrix for the first generation in the charged lepton sector in analogy with [10, 12]. This mass matrix includes the zero and first level KK modes and acquires the following form: [10]

$$\frac{\hat{\mathbf{M}}_e^{KK}}{(M_{KK})} = \begin{pmatrix} \bar{\ell}_L^{e(0)} \\ \bar{\ell}_L^{e(1)} \\ \bar{e}_L^{(1--)} \\ \bar{e}_L^{(1+-)} \end{pmatrix}^T \begin{pmatrix} \check{y}_e F_\ell F_e r_{00} x & 0 & \check{y}_e F_\ell r_{01} x & \check{y}_\nu F_\ell r_{101} x \\ \check{y}_e F_e r_{10} x & 1 & \check{y}_e^* r_{22} x & \check{y}_\nu r_{111} x \\ 0 & \check{y}_e r_{11} x & 1 & 0 \\ 0 & \check{y}_\nu^* r_{222} x & 0 & 1 \end{pmatrix} \begin{pmatrix} e_R^{(0)} \\ \ell_R^{e(1--)} \\ e_R^{(1)} \\ \bar{e}_R^{(1+-)} \end{pmatrix}, \quad (32)$$

where we factorized a common KK mass scale $M_{KK} \simeq 2.45 \Lambda_{IR}$, $\check{y}_{e,\nu} \equiv 2y_{e,\nu} v_\Phi^4 / \Lambda_{IR}$ and the perturbative expansion parameter is defined as $x \equiv v/M_{KK}$. In the above equation the various r 's denote the ratio of the bulk and IR localized effective couplings of the modes corresponding to the matrix element in question. For simplicity, we define $r_{111} \equiv r_{11-+}$, $r_{101} \equiv r_{01-+}$, $r_{22} \equiv r_{1-1-}$, $r_{222} \equiv r_{1-1+-}$ and the notation for the rest of the overlaps is straightforward [10]. The associated Yukawa matrix, \hat{Y}_{KK}^e , is obtained by simply eliminating x and the 1's from the above matrix and once rotated to the mass basis it describes the physical coupling between $(++)$, $(--)$, $(+-)$ and $(-+)$ KK modes. In [10] we have performed an analytical diagonalization of all one-generation zero+KK mass matrices in the quark sector and showed that the mild differences between the generations, stem from the structure of the 5D Yukawa couplings and non degeneracy of the RH bulk mass parameters.

The full three generation mass matrix will be 12×12 and of similar structure, which is modified mainly by the A_4 flavor structure. We first decompose the 12×12 mass matrix of the RS- A_4 charged lepton sector in terms of the one-generation KK+zero matrices in Eq. (32)

$$\hat{\mathbf{M}}_{Full}^\ell = M_{KK} \begin{pmatrix} \hat{\mathbf{M}}_e^{KK}/M_{KK} & x \hat{Y}_{KK}^\mu(\hat{y}_{12}^{LO}, F_\mu) & x \hat{Y}_{KK}^\tau(\hat{y}_{13}^{LO}, F_\tau) \\ x \hat{Y}_{KK}^e(\hat{y}_{21}^{LO}, F_e) & \hat{\mathbf{M}}_\mu^{KK}/M_{KK} & x \hat{Y}_{KK}^\tau(\hat{y}_{23}^{LO}, F_\tau) \\ x \hat{Y}_{KK}^e(\hat{y}_{31}^{LO}, F_e) & x \hat{Y}_{KK}^\mu(\hat{y}_{32}^{LO}, F_\mu) & \hat{\mathbf{M}}_\tau^{KK}/M_{KK} \end{pmatrix}, \quad (33)$$

where the expression in parenthesis for each off-diagonal element denotes the replacements to be made in Eq. (32) and the $\hat{M}_{\mu,\tau}^{KK}$ matrices are of exactly the same structure in Eq. (32). To account for NLO Yukawa interactions, the replacement $\hat{y}_{ij}^{LO} \rightarrow \hat{y}_{ij}^{LO} + \hat{y}_{ij}^{NLO}$ for the dimensionless 5D Yukawa coupling matrices applies. In the above equation, M_{KK} is the KK mass corresponding to the degenerate left-handed bulk mass parameter, c_ℓ^L , and we normalize all matrices accordingly while still keeping the small non-degeneracy of the KK masses, $M_{KK} \equiv M_{KK}^{\ell(1)} \simeq M_{KK}^{\tau(1)} \simeq 0.87M_{KK}^{e(1)} \simeq 0.95M_{KK}^{\mu(1)} \simeq 1.08M_{KK}^{\tilde{e}(1)}$. Finally, $v_\Phi^{4D}/\Lambda_{IR} \simeq 0.27$ and we assign $c_\ell \simeq c_\tau \simeq 0.51$, $c_e \simeq 0.787$, $c_\mu \simeq 0.63$, $y_e \simeq 1.2$, $y_\mu \simeq 1.55$ and $y_\tau \simeq 1.7$ to reproduce the charged lepton masses with an IR scale $\Lambda_{IR} \simeq 1.5$ TeV. The resulting masses are $m_e = 0.511$ MeV, $m_\mu = 105.7$ MeV and $m_\tau = 1.77$ GeV.

The reason fermion KK mixing is so important for off diagonal Z couplings is the presence of opposite chirality ($--$) KK states and “fake” custodial partners, which are the $SU(2)_R$ partners of ν_R (Eq. (1)) with $(-+)$ and $(+-)$ boundary conditions. Recall that a 5D fermion corresponds to two chiral fermions in 4D. As a result we will have LH states which couple to the Z boson as RH states (e.g. $\ell_R^{(1--)}$) and vice versa (e.g. $\tilde{e}_L^{(1+-)}$). As a result, the Z coupling matrices, $A_{L,R}(Z)$, which are proportional to the identity matrix in the ZMA (up to small deviations induced by Eq. (28)), contain instead both types of (diagonal) entries (g_L^Z) $_{SM}$, (g_R^Z) $_{SM}$ and will thus acquire non vanishing off diagonal elements, once rotated to the common mass basis of the KK and zero mode fermions.

Unfortunately, the three generation charged lepton (KK+zero) mass matrix can only be diagonalized numerically, due to its dimension and the large number of input parameters. The numerical diagonalization of this matrix is quite involved due to the presence of large hierarchies, ranging from m_e to M_{KK} . It is thus essential to obtain an analytical approximation for $(\delta g_{L,R}^{\mu e})_{KK}$, to get a control over the numerical results. For this purpose, we follow [36] and use an effective field theory approach, where all heavy modes are integrated out. Within this approximation the zero mode mass matrix is modified in the following way,

$$(M_{00})^{KK} = M_{00} + M_{0k}M_k^{-1}M_{kj}M_j^{-1}M_{j0} - \frac{1}{2} \left[M_{0k}M_k^{-2}M_{0k}^\dagger M_{00} + M_{00}M_{k0}^\dagger M_k^{-2}M_{k0} \right] + \dots, \quad (34)$$

where the first correction originates from the pure heavy (KK) mass terms, while the second correction containing M_{00} is generated by the redefinitions of the light (SM) charged lepton fields, which are required to bring the kinetic terms into their canonical form [36]. Notice that M_{00} is precisely the ZMA mass matrix given in Eq. (6), upon the identification $y_{e,\mu,\tau}^{4D} \equiv 2y_{e,\mu,\tau}F_\ell F_{e,\mu,\tau}(v_\Phi^{4D}/\Lambda_{IR})r_{00}^{e,\mu,\tau}$. In Eq. (34) the zero+KK mass matrix of Eq.(33) is decomposed into its “generational” 3×3 building blocks, such that M_{kj} is obtained by taking the (kj) element of each of the 4×4 block matrices in Eq. (33). To simplify the notation, we label the zero and KK modes in the basis vectors of Eq. (32) as $(0, 1, 2, 3)$. Observing Eq. (32), we immediately realize that $M_{01} = M_{20} = M_{30} = M_{23} = M_{32} = 0$, $M_{11,33} = \mathbb{1} \cdot M_{KK}^{\ell(1),\tilde{e}(1)}$ and $M_{22} = \text{diag}(M_{KK}^{e(1),\mu(1),\tau(1)})$.

The modified mass matrix of Eq.(34) induces corrections to the left and right handed Z coupling matrices for the zero modes, $[A_{L,R}(Z)]_{00}$, where the first non vanishing corrections

can be thought of as coming from placing two KK-zero mass insertions on the fermionic legs of a $Z f_{L,R}^{(0)} f_{L,R}^{(0)}$ vertex. The corrected coupling matrices are given by [36]

$$[A_L(Z)]_{00}^{KK} = [A_L(Z)]_{00} + M_{0k} M_k^{-2} [A_L(Z)]_{kk} M_{0k}^\dagger - \frac{1}{2} \left[M_{0k} M_k^{-2} M_{0k}^\dagger [A_L(Z)]_{00} + [A_L(Z)]_{00} M_{00} M_{0k} M_k^{-2} M_{0k}^\dagger \right] + \dots, \quad (35)$$

$$[A_R(Z)]_{00}^{KK} = [A_R(Z)]_{00} + M_{k0}^\dagger M_k^{-2} [A_R(Z)]_{kk} M_{k0} - \frac{1}{2} \left[M_{k0}^\dagger M_k^{-2} M_{k0} [A_R(Z)]_{00} + [A_R(Z)]_{00} M_{00} M_{k0}^\dagger M_k^{-2} M_{k0} \right] + \dots \quad (36)$$

In the above equations, the corrected coupling matrices $[A_{L,R}(Z)]_{00}^{KK}$ are given in the interaction basis and should be rotated to the physical basis by the usual transformation $(V_{L,R}^\ell)^\dagger [A_{L,R}]_{00}^{KK} V_{L,R}^\ell$. To account solely for KK mixing effects we ignore the small deviations implied by Eq.(28), such that $[A_{L,R}(Z)]_{00} = (g_{L,R}^Z)^{SM} \cdot \mathbb{1}$, $[A_{L,R}]_{11} = (g_L^Z)_{SM} \cdot \mathbb{1}$ and $[A_{L,R}(Z)]_{22,33} = (g_R^Z)_{SM} \cdot \mathbb{1}$. To account for gauge boson mixing effects, we simply replace the first (zero order) terms in Eqs. (35) and (36) by $[A_{L,R}(Z)]_{00}^G$ of Eqs. (29) and (30).

We are now ready to compute the corrections to $\delta(g_{L,R}^{\mu e})_{SM} = 0$ from fermion KK mixing. Starting from $A_L(Z)$ and using $M_{01} = 0$ and $[A_{L,R}(Z)]_{22,33} = (g_R^Z)_{SM} \cdot \mathbb{1}$ we have:

$$A_L(Z) = [A_L(Z)]_{00} + ((g_R^Z)_{SM} - (g_L^Z)_{SM}) \left[M_{02} M_{22}^{-2} M_{02}^\dagger + M_{03} M_{33}^{-2} M_{03}^\dagger \right], \quad (37)$$

where $(g_R^Z)_{SM} - (g_L^Z)_{SM} = 1/2$. The block matrices M_{02} and M_{03} inherit their structure from the 5D Yukawa Lagrangian and are given by:

$$M_{02} = \begin{pmatrix} (\check{y}_e + \check{x}_1^\ell f_\chi^e) F_\ell r_{01}^e x & (\check{y}_\mu + \check{x}_2^\ell f_\chi^\mu) F_\ell r_{01}^\mu x & (\check{y}_\tau + \check{x}_3^\ell f_\chi^\tau) F_\ell r_{01}^\tau x \\ \check{y}_e F_e r_{01}^e x & \omega \check{y}_\mu F_\ell r_{01}^\mu x & \omega^2 \check{y}_\tau F_\ell r_{01}^\tau x \\ (\check{y}_e + x_1^e f_\chi^e) F_\ell r_{01}^e x & (\omega^2 \check{y}_\mu + \check{y}_2^\ell f_\chi^\mu) F_\ell r_{01}^\mu x & (\omega \check{y}_\tau + \check{y}_3^\ell f_\chi^\tau) F_\ell r_{01}^\tau x \end{pmatrix}, \quad (38)$$

$$M_{03} = \begin{pmatrix} (\check{y}_\nu + \check{\epsilon}_1) F_\ell r_{101}^\nu x & \check{\epsilon}_2 F_\ell r_{101}^\nu x & (\check{\epsilon}_3 + \check{\epsilon}_\chi) F_\ell r_{101}^\nu x \\ \check{\epsilon}_3 F_\ell r_{101}^\nu x & (\check{y}_\nu + \check{\epsilon}_1) F_\ell r_{101}^\nu x & \check{\epsilon}_2 F_\ell r_{101}^\nu x \\ (\check{\epsilon}_2 + \check{\epsilon}_\chi) F_\ell r_{101}^\nu x & \check{\epsilon}_3 F_\ell r_{101}^\nu x & (\check{y}_\nu + \check{\epsilon}_1) F_\ell r_{101}^\nu x \end{pmatrix}. \quad (39)$$

We expect the most dominant contribution to come from the term proportional to $M_{03} M_{33}^{-2} M_{03}^\dagger$ induced by the interactions of the LH zero modes $\ell_L^{(0)e,\mu,\tau}$ with the ‘‘custodians’’ $(\check{e}_R^{(1+-)}, \check{\mu}_R^{(1+-)}, \check{\tau}_R^{(1+-)})$. Since $\check{\epsilon}_{1,2,3}$ come from the Z_3 preserving 5D operator $k^{-7/2} \bar{\ell}_L H \Phi^2 \nu_R$, we expect them to be ‘‘rotated away’’ with V_L^ℓ at $\mathcal{O}(\epsilon_{1,2,3,\chi}, f_\chi)$ and indeed using $M_{33} = M_{KK}^{\check{\epsilon}^{(1+-)}} \cdot \mathbb{1}$ and Eq. (7), we factorize out $(F_\ell r_{101}^\nu)^2 v^2 / (M_{KK}^{\check{\epsilon}^{(1+-)}})^2$ and obtain:

$$(V_L^\ell)^\dagger M_{03} M_{33}^{-2} M_{03}^\dagger V_L^\ell \propto \begin{pmatrix} |\check{y}_\nu|^2 + \frac{4}{3} \text{Re}(\check{y}_\nu \check{\epsilon}_\chi) & -\frac{2\omega}{3} \text{Re}(\check{y}_\nu \check{\epsilon}_\chi) & -\frac{2\omega^2}{3} \text{Re}(\check{y}_\nu \check{\epsilon}_\chi) \\ -\frac{2\omega^2}{3} \text{Re}(\check{y}_\nu \check{\epsilon}_\chi) & |\check{y}_\nu|^2 - \frac{2}{3} \text{Re}(\check{y}_\nu \check{\epsilon}_\chi) & \frac{4\omega}{3} \text{Re}(\check{y}_\nu \check{\epsilon}_\chi) \\ -\frac{2\omega}{3} \text{Re}(\check{y}_\nu \check{\epsilon}_\chi) & \frac{4\omega^2}{3} \text{Re}(\check{y}_\nu \check{\epsilon}_\chi) & |\check{y}_\nu|^2 - \frac{2}{3} \text{Re}(\check{y}_\nu \check{\epsilon}_\chi) \end{pmatrix}. \quad (40)$$

The above expression is already given in the mass basis and to get the contribution to the $Z\mu e$ coupling we simply take the (12) element of the matrix in Eq. (40), recalling the prefactors:

$$\delta(g_L^{\mu e})_{\tilde{K}K}^{(1)} \simeq \left| \frac{-\omega}{3} \text{Re}(\check{y}_\nu \check{\epsilon}_\chi) (F_\ell r_{101}^\nu)^2 \frac{v^2}{(M_{KK}^{\tilde{e}(1+-)})^2} \right| \approx 9 \times 10^{-8}, \quad (41)$$

where we used $r_{101}^\nu \simeq 0.72$, $F_\ell \simeq 0.1$ and set $|y_{\nu, \epsilon_\chi}| = 1$. We now proceed to obtain the correction coming from the $M_{02} M_{22}^{-2} M_{02}^\dagger$ term in Eq. (37). We expect this term to generate a suppressed contribution due to the approximate alignment of M_{02} and M_{00} . Notice that due to the degeneracy of c_ℓ , we can write M_{02} as

$$M_{02} = M_{00} \text{diag} [F_{e,\mu,\tau}^{-1} (r_{00}^{e,\mu,\tau})^{-1} r_{01}^{e,\mu,\tau}], \quad (42)$$

using this compact form it is straightforward to transform this correction to the mass basis:

$$\begin{aligned} (V_L^\ell)^\dagger M_{02} M_{22}^{-2} M_{02}^\dagger V_L^\ell &= (V_L^\ell)^\dagger M_{00} V_R^\ell (V_R^\ell)^\dagger \text{diag} \left(\frac{(r_{01}^{e,\mu,\tau})^2}{(F_{e,\mu,\tau} r_{00}^{e,\mu,\tau} M_{KK}^{e(1),\mu(1),\tau(1)})^2} \right) V_R^\ell (V_R^\ell)^\dagger M_{00}^\dagger V_L^\ell \\ &= \text{diag}(m_{e,\mu,\tau}) (V_R^\ell)^\dagger \text{diag} \left(\frac{(r_{01}^{e,\mu,\tau})^2}{(F_{e,\mu,\tau} r_{00}^{e,\mu,\tau} M_{KK}^{e(1),\mu(1),\tau(1)})^2} \right) V_R^\ell \text{diag}(m_{e,\mu,\tau}) \\ &= m_{e_i} m_{e_j} \sum_{n=1}^3 (V_R)_{ni}^* (V_R)_{nj} \left(\frac{(r_{01}^{e,\mu,\tau})^2}{(F_{e,\mu,\tau} r_{00}^{e,\mu,\tau} M_{KK}^{e(1),\mu(1),\tau(1)})^2} \right)_{nn}. \end{aligned} \quad (43)$$

It is now straight forward to estimate $(\delta g_L^{\mu e})_{\tilde{K}K}^{e_i(1)}$ by taking the (12) element from the above expression. The dominant term acquires the form:

$$(\delta g_L^{\mu e})_{\tilde{K}K}^{e_i(1)} \simeq \frac{m_e m_\mu \Delta_1^\ell (r_{01}^\mu)^2}{(F_\mu r_{00}^\mu M_{KK}^{\mu(1)})^2} \approx 6 \times 10^{-11}, \quad (44)$$

where we set all Yukawas to 1 in magnitude and use $F_\mu \simeq 0.004$, $r_{01}^\mu \simeq 0.8$ and $r_{00}^\mu \simeq 0.87$. This concludes the calculation of KK fermion mixing contribution to $\delta g_L^{\mu e}$.

We now turn to the RH couplings, in which case we have only one term contributing, proportional to $M_{10}^\dagger M_{11}^{-2} M_{10}$ and thus Eq. (36) simplify to:

$$A_R(Z) = [A_R(Z)]_{00} + ((g_L^Z)_{SM} - (g_R^Z)_{SM}) \left[M_{10}^\dagger M_{11}^{-2} M_{10} \right], \quad (45)$$

where $(g_L^Z)_{SM} - (g_R^Z)_{SM} = -1/2$, $M_{11} = M_{KK}^{\ell(1)} \cdot \mathbb{1}$ and the various entries of M_{10} are given by

$$M_{10} = \begin{pmatrix} (\check{y}_e + \check{x}_1^\ell f_\chi^e) F_e r_{10}^e x & (\check{y}_\mu + \check{x}_2^\ell f_\chi^\mu) F_\mu r_{10}^\mu x & (\check{y}_\tau + \check{x}_3^\ell f_\chi^\tau) F_\tau r_{10}^\tau x \\ \check{y}_e F_e r_{10}^e x & \omega \check{y}_\mu F_\mu r_{10}^\mu x & \omega^2 \check{y}_\tau F_\tau r_{10}^\tau x \\ (\check{y}_e + x_1^e f_\chi^e) F_e r_{10}^e x & (\omega^2 \check{y}_\mu + \check{y}_2^\ell f_\chi^\mu) F_\mu r_{01}^\mu x & (\omega \check{y}_\tau + \check{y}_3^\ell f_\chi^\tau) F_\tau r_{10}^\tau x \end{pmatrix}. \quad (46)$$

Once again, the degeneracy of c_ℓ implies that M_{10} is approximately aligned with M_{00} and can be written in the following way:

$$M_{10} = M_{00} \text{diag}(r_{10}^{e,\mu,\tau}/r_{00}^{e,\mu,\tau}) F_\ell^{-1}. \quad (47)$$

The above equation simplifies the transformation of Eq. (45) to the mass basis and we get:

$$\begin{aligned} (V_R^\ell)^\dagger M_{10}^\dagger M_{11}^{-2} M_{10} V_R^\ell &= (V_R^\ell)^\dagger \text{diag} \left(\frac{r_{10}^{e,\mu,\tau}}{r_{00}^{e,\mu,\tau}} \right) V_R^\ell (V_R^\ell)^\dagger M_{00}^\dagger V_L^\ell \\ &\cdot (V_L^\ell)^\dagger M_{00} V_R^\ell (V_R^\ell)^\dagger \text{diag} \left(\frac{r_{10}^{e,\mu,\tau}}{(M_{KK}^{\ell(1)})^2 r_{00}^{e,\mu,\tau}} \right) V_R^\ell. \end{aligned} \quad (48)$$

We use the same steps taken for the LH couplings in Eq. (43) to simplify the long expression in Eq. (48). The resulting expression for $[\Delta A_R]^{mass} \equiv (V_R^\ell)^\dagger M_{10}^\dagger M_{11}^{-2} M_{10} V_R^\ell$ reads,

$$[\Delta A_R]_{ij}^{mass} = F_\ell^{-2} \left[\sum_{n,k,l=1}^3 (V_R^\ell)_{ni}^* (V_R^\ell)_{nk} (m_{e_k})^2 \text{diag} \left(\frac{r_{10}^{e,\mu,\tau}}{r_{00}^{e,\mu,\tau}} \right)_{nn} (V_R^\ell)_{lk}^* (V_R^\ell)_{lj} \text{diag} \left(\frac{r_{10}^{e,\mu,\tau}}{r_{00}^{e,\mu,\tau}} \right)_l \right]. \quad (49)$$

We realize that due to the degeneracy of c_ℓ the LH diagonalization matrices are absent in the above expression, implying that the off diagonal elements of $[\Delta A_R]_{ij}^{mass}$ will come from terms proportional to the NLO corrections of V_R^ℓ and will also consist of additional cancellation patterns, induced by the near degeneracy of the Higgs-flavon overlap correction factors $r_{10,00}^{e,\mu,\tau}$. Specifying to the RH $Z\mu e$ coupling, we extract the dominant terms and obtain

$$(\delta g_R^{\mu e})_{KK}^{\ell(1)} \simeq F_\ell^{-2} \left[\frac{m_\mu^2 \Delta_1^\ell r_{10}^\mu}{(M_{KK}^{\ell(1)})^2 r_{00}^\mu} \left(\frac{r_{10}^e}{r_{00}^e} - \frac{r_{10}^\mu}{r_{00}^\mu} \right) \right] + \dots \approx 10^{-12}, \quad (50)$$

where we have omitted terms, which are at least $\mathcal{O}(f_\chi \approx 0.05)$ suppressed compared to those appearing in the above equation. To get the numerical estimation, we assigned all Yukawas to 1 and used $r_{00}^e \simeq 0.895$, $r_{00}^\mu \simeq 0.87$, $r_{00}^\tau \simeq 0.86$, $r_{10}^e \simeq 0.754$, $r_{10}^\mu \simeq 0.74$ and $r_{10}^\tau \simeq 0.73$. To summarize our analytical estimations we have:

$$(\delta g_L^{\mu e})^{gauge} = 0, \quad (\delta g_L^{\mu e})^{KK} \approx 9 \times 10^{-8}, \quad (\delta g_R^{\mu e})^{gauge} \approx 5 \times 10^{-11}, \quad (\delta g_R^{\mu e})^{KK} \approx 10^{-12}. \quad (51)$$

4.3 FCNC protection in the brane localized RS-A₄ setup

Since both the gauge and fermionic contributions, calculated in the previous sections, come from ‘‘cross-brane’’ effects it seems natural to believe that the brane localized RS-A₄ setup

is completely protected from all sources of tree level FCNC. This point was discussed in [5], yet the fermion KK mixing effects, were not taken into account there. Indeed, in the brane localized case we have $V_R^\ell = \mathbb{1}$, which together with the degeneracy of c_ℓ implies there can be no gauge boson mixing induced contributions to tree level FCNC (Eq. (30)). Similarly, the analytical approximations for $(\delta g_{L,R}^{\mu e})^{KK}$ (Eqs. (41), (44) and (49)) suggest that these sources of FCNC are turned off as well. Going to higher order in the expansion of Eqs. (35) and (36) won't do the trick since all blocks of the KK+zero mass matrix inherit their structure from the 5D Yukawa lagrangian, which is "form diagonal" in the brane localized case. Due to the Z_3 preserving VEV of Φ (Eq. (5), the interactions with the custodians $(\tilde{e}^{(1)}, \tilde{\mu}^{(1)}, \tilde{\tau}^{(1)})$, which mimic the Dirac interactions in the neutrino sector, are also "form diagonalizable", namely, diagonalized by $U(\omega)$ (Eq. (6)) and thus can not contribute to FCNC.

The absence of tree level FCNC is not surprising since the LH zero modes are degenerate and the RH zero modes require no rotation to be transformed into the mass basis. This means that one can always find a basis in which the kinetic and mass terms are simultaneously diagonal, which simply forbids FCNC. Nevertheless, we have shown in the context of one loop contributions to dipole operators in the quark sector [10], that the degeneracy between the KK masses, which is even stronger in the charged lepton sectors, implies that a non perturbative rotation of the degenerate KK blocks is needed before we can act with standard techniques of non-degenerate perturbation theory. Such a rotation, mixes the KK states maximally with each other (generation+BC) and might still induce small contributions to tree level FCNC. To verify the extent to which such a situation contributes to FCNC we shall attempt to analytically diagonalize the zero+first KK modes mass matrix. This seemingly hard task, shall be greatly simplified due to the magic properties of $U(\omega)$. We start by writing the 9×9 KK-KK block of the full mass matrix in terms of 3×3 building blocks,

$$\mathbf{M}_{KK}^{9 \times 9} \propto \begin{pmatrix} M_{KK}^{\ell(1)} \cdot \mathbb{1} & \sqrt{3}U(\omega)\text{diag}(y_{e,\mu,\tau} r_{11}^{e,\mu,\tau})v & \hat{Y}_{KK}^\nu r_{111}^\nu v \\ \sqrt{3}U(\omega)\text{diag}(y_{e,\mu,\tau}^* r_{22}^{e,\mu,\tau})v & \text{diag}\left(M_{KK}^{e(1),\mu(1),\tau(1)}\right) & 0 \\ (\hat{Y}_{KK}^\nu)^\dagger r_{222}^\nu v & 0 & M_{KK}^{\tilde{e}(1+^-)} \cdot \mathbb{1} \end{pmatrix}, \quad (52)$$

where $v = 174 \text{ GeV}$ is the Higgs VEV and \hat{Y}_ν^{KK} is a dimensionless coupling matrix, inheriting its structure from the Dirac neutrino mass matrix (Eq. (13)) and is given by:

$$\hat{Y}_\nu^{KK} = \begin{pmatrix} y_\nu + \epsilon_1 & \epsilon_2 & \epsilon_3 \\ \epsilon_3 & y_\nu + \epsilon_1 & \epsilon_2 \\ \epsilon_2 & \epsilon_3 & y_\nu + \epsilon_1 \end{pmatrix}. \quad (53)$$

Because of the symmetry between the $\epsilon_{2,3}$ entries, which is inherited from the Z_3 preserving VEV of Φ , we expect \hat{Y}_ν^{KK} to be diagonalized by $U(\omega)$ and indeed we realize that:

$$\hat{Y}_\nu^{KK} = U(\omega) \underbrace{\begin{pmatrix} y_\nu + \epsilon_1 + \epsilon_2 + \epsilon_3 & 0 & 0 \\ 0 & y_\nu + \epsilon_1 + \omega\epsilon_2 + \omega^2\epsilon_3 & 0 \\ 0 & 0 & y_\nu + \epsilon_1 + \omega^2\epsilon_2 + \omega\epsilon_3 \end{pmatrix}}_{\hat{Y}_\nu^{KK(diag.)}} (U(\omega))^\dagger. \quad (54)$$

Observing the above features of $U(\omega)$, we realize that the first trivial rotation we can impose on the KK mass matrix of Eq. (52), will be block diagonal, where each 3×3 building block is identified with either $U(\omega)$ or the identity matrix. Such a rotation will leave the Z coupling matrices, $A_{L,R}(Z)$ unchanged, since each 3×3 block in $A_{L,R}(Z)$ is proportional to the identity. In particular consider, the matrix $U_{L[R]}^{12 \times 12} = \text{diag}[U(\omega)[\mathbb{1}], \mathbb{1}, U(\omega), U(\omega)]$. Acting with $U_L^{12 \times 12}$ on $\hat{\mathbf{M}}_{Full}^\ell$ will make each 3×3 block generation diagonal, which means that the nine dimensional degenerate subspace, which had to be diagonalized has splitted into three, according to the ‘‘type’’ (BC) of KK modes. Assuming the degeneracy of KK masses, the rotated KK+zero mass matrix, $\hat{\mathbf{M}}_{Full}^{\ell(U)}$ is proportional to:

$$\begin{pmatrix} \text{diag}(\check{y}_{e,\mu,\tau} F_\ell F_{e,\mu,\tau} r_{00}^{e,\mu,\tau}) & 0 & \text{diag}(\check{y}_{e,\mu,\tau} F_{e,\mu,\tau} (r_{01}^{e,\mu,\tau})) & \check{Y}_{KK}^{\nu(diag.)} F_\ell r_{10}^\nu \\ \text{diag}(\check{y}_{e,\mu,\tau} F_{e,\mu,\tau} r_{10}^{e,\mu,\tau}) & 1/x & \text{diag}(\check{y}_{e,\mu,\tau} r_{11}^{e,\mu,\tau}) & \check{Y}_{KK}^{\nu(diag.)} F_\ell r_{11}^\nu \\ 0 & \text{diag}(\check{y}_{e,\mu,\tau}^* r_{22}^{e,\mu,\tau}) & 1/x & 0 \\ 0 & \check{Y}_{KK}^{\nu(diag.)\dagger} F_\ell r_{22}^\nu & 0 & 1/x \end{pmatrix}, \quad (55)$$

where $x = v/M_{KK}$. We realize that all 3×3 blocks of the above matrix are diagonal, namely we can treat each blocks as a set of three complex numbers, without worrying about the inversion of parametric 3×3 matrices. Recalling the independence of $U(\omega)$ from the LO Yukawa couplings, we realize that the 9×9 KK block of the matrix in Eq. (55) has the characteristic form:

$$\left(\hat{\mathbf{M}}_{Full}^\ell(U) \right)_{9 \times 9}^{KK} \propto M_{KK}^{ch.} \equiv \begin{pmatrix} 1/x & A & B \\ aA^* & 1/x & 0 \\ bB^* & 0 & 1/x \end{pmatrix}, \quad (56)$$

where $A \equiv \text{diag}(\check{y}_{e,\mu,\tau} r_{11}^{e,\mu,\tau})$, $B = \check{Y}_{KK}^{\nu(diag.)} F_\ell r_{11}^\nu$ and $\hat{a}(\hat{b}) = \text{diag}(r_{22(222)}^{e,\mu,\tau(\nu)}/r_{11(111)}^{e,\mu,\tau(\nu)})$. Using $r_{11}^e \simeq 0.763$, $r_{11}^\mu \simeq 0.758$, $r_{11}^\tau \simeq 0.753$, $r_{111}^\nu \simeq 0.749$, $r_{22}^e \simeq 0.383$ and $r_{22}^\mu \simeq 0.367$, $r_{22}^\tau \simeq 0.357$ and $r_{222}^\nu \simeq 0.19$, we realize that $\hat{a} \simeq \hat{b} \simeq 1/2 \cdot \mathbb{1}$. The resulting $M_{KK}^{ch.}$ can be diagonalized analytically by the transformation, $M_{KK}^{ch.(diag.)} = (V_L^{KK})^\dagger M_{KK}^{ch.} V_R^{KK}$, where $V_{L,R}^{KK}$ are given by:

$$V_{L,R}^{KK} = \begin{pmatrix} 0 & -\frac{e^{\pm i\theta_B}}{\sqrt{2}} & \frac{e^{\pm i\theta_B}}{\sqrt{2}} \\ -\frac{|B|e^{\pm i(\theta_B - \theta_A)}}{\sqrt{|A|^2 + |B|^2}} & \frac{|A|e^{\pm i(\theta_B - \theta_A)}}{\sqrt{2(|A|^2 + |B|^2)}} & \frac{|A|e^{\pm i(\theta_B - \theta_A)}}{\sqrt{2(|A|^2 + |B|^2)}} \\ \frac{|A|}{\sqrt{|A|^2 + |B|^2}} & \frac{|B|}{\sqrt{2(|A|^2 + |B|^2)}} & \frac{|B|}{\sqrt{2(|A|^2 + |B|^2)}} \end{pmatrix}, \quad (57)$$

and where $M_{KK}^{ch.(diag.)} = \text{diag} \left(1, 1 - 3/2\sqrt{|A|^2 + |B|^2}, 1 + 3/2\sqrt{|A|^2 + |B|^2} \right)$. We are now left only with the non vanishing zero-KK blocks – they are mixtures of the flavor diagonal blocks, $\text{diag}(\check{y}_{e,\mu,\tau} F_{e,\mu,\tau(\ell)} r_{01(10)}^{e,\mu,\tau})$ and $\hat{Y}_{KK}^{\nu(diag.)} F_{\ell} r_{101}^{\nu}$. Therefore, the remaining (standard) perturbative diagonalization of $M_{KK}^{ch.(diag.)}$ won't contribute to FCNC, to all orders. If we will consider the explicit values of the overlap correction factors, r_{nm} above, flavor violating couplings may be generally generated at $\mathcal{O}(v^4/M_{KK}^4)$, but will be further suppressed by quartic differences of the nearly degenerate r_{nm} . Such contributions are negligibly small ($\mathcal{O}(10^{-18})$) and will thus not be further discussed. Finally, it is important to stress that the above diagonalization scheme can be easily generalized to include an arbitrary number of KK modes and will yield the same results in this case.

4.4 The RS-A₄ contributions to $\mu \rightarrow 3e$ and $\mu \rightarrow e$ conversion

The effective Lagrangian for $\mu \rightarrow 3e$ decay and $\mu \rightarrow e$ conversion in nuclei is written in terms of four fermion operators. These lepton flavor-violating Fermi operators are traditionally parametrized as [37]

$$\begin{aligned} \mathcal{L} = & \frac{4G_F}{\sqrt{2}} [g_3(\bar{e}_R\gamma^\mu\mu_R)(\bar{e}_R\gamma_\mu e_R) + g_4(\bar{e}_L\gamma^\mu\mu_L)(\bar{e}_L\gamma^\mu e_L) + g_5(\bar{e}_R\gamma^\mu\mu_R)(\bar{e}_L\gamma_\mu e_L) \\ & + g_6(\bar{e}_L\gamma^\mu\mu_L)(\bar{e}_R\gamma_\mu e_R)] + \frac{G_F}{\sqrt{2}} \bar{e}\gamma^\mu(v - a\gamma_5)\mu \sum_q \bar{q}\gamma_\mu(v^q - a^q\gamma_5)q, \end{aligned} \quad (58)$$

where in the normalization we use, $v^q = T_3^q - 2Q^q \sin^2\theta$. The axial coupling to quarks, a^q , vanishes in the dominant contribution coming from coherent scattering off the nucleus. The $g_{3,4,5,6}$ are responsible for $\mu \rightarrow 3e$ decay, while the v, a are responsible for $\mu \rightarrow e$ conversion in nuclei. The rates are given by (with the conversion rate normalized to the muon capture rate):

$$\text{Br}(\mu \rightarrow 3e) = 2(g_3^2 + g_4^2) + g_5^2 + g_6^2, \quad (59)$$

$$\text{Br}(\mu \rightarrow e) = \frac{p_e E_e G_F^2 F_p^2 m_\mu^3 \alpha^3 Z_{eff}^4}{\pi^2 Z \Gamma_{\text{capt}}} Q_N^2 (v^2 + a^2), \quad (60)$$

where the parameters for the conversion depend on the nucleus and are calculated in the Feinberg-Weinberg approximation [38] and we write the charge for a nucleus with atomic number Z and neutron number N as

$$Q_N = v^u(2Z + N) + v^d(2N + Z). \quad (61)$$

The most sensitive experimental constraint, $\text{Br}(\mu \rightarrow e) \lesssim 6 \times 10^{-13}$, comes from muon conversion in ${}^{48}_{22}\text{Ti}$ [21], for which

$$E_e \sim p_e \sim m_\mu, \quad F_p \sim 0.55, \quad Z_{\text{eff}} \sim 17.61, \quad \Gamma_{\text{capt}} \sim 2.6 \cdot \frac{10^6}{\text{s}}. \quad (62)$$

Using these couplings one can estimate the coefficients of the 4-Fermi operators in (58),

$$g_{3,4} = 2(\delta g_{L,R}^{\mu e})^2 \quad g_{5,6} = 2\delta g_L^{\mu e} \delta g_R^{\mu e} \quad (v \pm a) = 2\delta g_{L,R}^{\mu e}, \quad (63)$$

where $\delta g_{L,R}^{\mu e}$ contains both the gauge and fermionic contributions to the $Z\mu e$ coupling.

Recalling our collective estimations of the gauge and fermionic contributions (Eq. (51)), obtained for Yukawa couplings with magnitude 1 and random phase, we have $(\delta g_{L(R)}^{\mu e})_{G+KK} \approx 8 \times 10^{-8} (5 \times 10^{-11})$. We expect the results of a numerical scan over the magnitudes and phases of the Yukawa couplings to be centered around these values if the effective field theory approach we used (Eq. (34)) is reliable. To find the exact result we perform a numerical diagonalization of $\hat{\mathbf{M}}_{Full}^\ell$ and use the resulting diagonalization matrices, $\mathbf{V}_{L,R}^{\mathbf{KK}(\text{full})}$ to rotate the 12×12 coupling matrices $A_{L,R}(Z) = \text{diag}([A_{L,R}(Z)]_{00,11,22,33})$ to the zero+KK mass basis, where we have $(\delta g_{L,R}^{Z\mu e})_{mass} = [A_{L,R}(Z)]_{\mu(0)e(0)}^{mass}$. Once we obtain $(\delta g_{L,R}^{Z\mu e})_{mass}^{RS-A_4}$ we perform a matching to the operators contributing to $\mu \rightarrow e, 3e$ (Eq. (58)) using Eqs. (59) and (60). Using the points satisfying the 3σ bounds on the neutrino mixing angles from the scan of Sec. 3, we generate a sample of 40000 points, consisting of the $\epsilon_{2,3,4,\chi}$, $\tilde{x}_{2,3}^\ell$ and $\tilde{y}_{2,3}^\ell$ parameters. The distribution of the values of each of these parameters, within the sample, is practically indistinguishable from the original distribution from which it was taken from. Namely, all parameters are still complex numbers with random phases and magnitudes normally distributed around 1 with standard deviation 0.5. Since $BR(\mu \rightarrow e, 3e) \propto (g_{L,R}^{Z\mu e})^2$ (Eqs. (59)–(60)) and δg_L generally dominates, we can plot the constraints coming from the various cLFV experiments as vertical lines in the $\delta g_L^{\mu e Z} - \delta g_R^{\mu e Z}$ plane. The results are depicted in Fig. 7 (left). The results of a separate scan, independent of constraints from the neutrino sector, reveal negligible differences and are thus not discussed separately. By observing Eqs. (20)–(22) we recall that all mixing angles receive contributions from four NLO Yukawa couplings in the charged lepton sector $\tilde{x}_{2,3}^\ell$ and $\tilde{y}_{2,3}^\ell$. Consequently, there are simply too many input parameters of $\mathcal{O}(1)$ and random phases, which can't be significantly constrained by the experimental data. By observing Fig. 7 we realize that the numerical results are in an excellent agreement with the estimations of Eq. (51). This strengthens our confidence in the effective field theory approach adopted from [36]. The current bound from SINDRUM II [21] “eliminates” around 35% of the cross-brane RS- A_4 setup and is easily and naturally satisfied for $\Lambda_{IR} \simeq 1.5 \text{ TeV}$. The correlation between the LH and RH $Z\mu e$ couplings is attributed to the fact that they are both generated by cross brane effects, induced by v_χ (Eq. (4)). When cross brane effects are neglected, the $Z\mu e$ couplings are negligible (right plot of Fig. 7), while corrections to the TBM pattern can only come from higher order corrections to the heavy Majorana and Dirac mass matrices. Recall that in this case, achieving $\theta_{13} \sim \theta_C/\sqrt{2}$ is slightly less natural from the 5D theory point of view (requires $|y_{e4}| \sim 6$) (Sec. 3.1). We conclude that if no $\mu \rightarrow e, 3e$ events will be actually observed in Mu3e, MuSIC and Dee-Mee the “cross talk” RS- A_4 model will be severely constrained and less appealing. On the other hand, the predictions for the brane localized realizations of RS- A_4 are extremely far from the reach of Mu2e [26], COMET [23], PRIME [24] and other future experiments. Most probably, the same situation will not hold true for the $\mu \rightarrow e\gamma$ decay induced at the one-loop level. The current upper bound is $\text{Br}(\mu \rightarrow e\gamma) \lesssim 6 \times 10^{-13}$ [39]

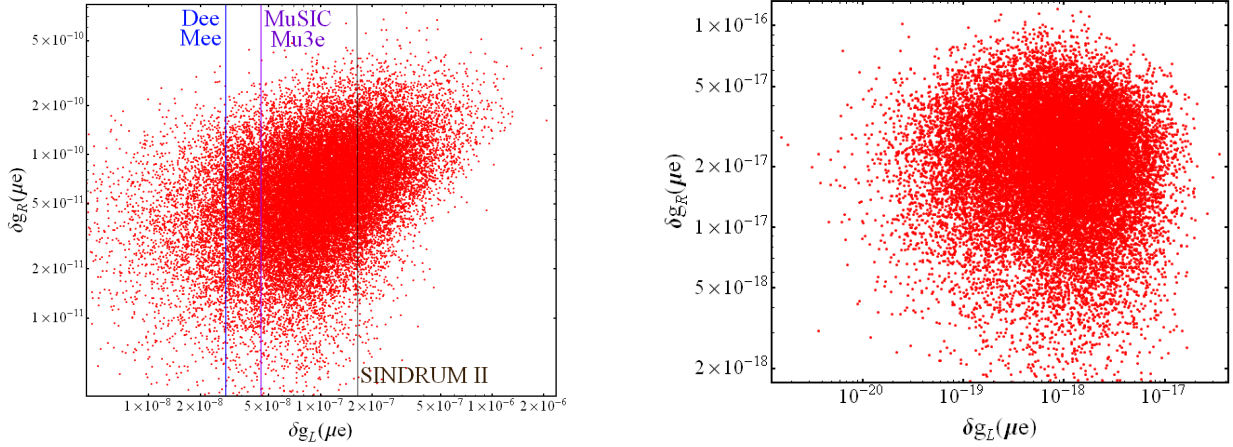


Figure 7: *The RS- A_4 predictions for the anomalous LH and RH $Z\mu e$ couplings in the presence (left) or absence (right) of cross brane interactions. Each point represents the contributions coming from both gauge boson mixing and KK fermion mixing, including all dominant higher order and cross talk effects. The dashed lines represent the maximum sensitivities of past, present and future LFV experiments taking place at FERMILAB and J-PARC.*

and is expected to improve by roughly two orders of magnitude in the next few years. This concludes our analysis of cLFV in RS- A_4 setups.

5 Conclusions

In this work we have studied the charged lepton and neutrino sectors of RS- A_4 (seesaw I) models excluding/including cross brane effects. For the neutrino sector, we have shown that cross-talk operators in the charged lepton sector and brane localized higher order corrections to the (heavy) Majorana and Dirac mass matrices induce significant deviations from TBM neutrino mixing, such that the experimental bounds can be rather easily satisfied. The mild differences between the normal and inverted hierarchy cases come from the terms proportional to $\epsilon_{2,3,4}$ in Eqs. (20)–(22), associated with brane localized higher dimensional operators in the neutrino sector. The success rates for satisfying the 3σ bounds from all mixing angles simultaneously were shown to be $\xi_{NH(IH)} \simeq 10\%(12.5\%)$, which is slightly higher than those associated with “typical” A_4 seesaw models [31] and with anarchic models [40]. Therefore, despite the fact that the recent measurements of $\theta_{13} \approx \lambda_C/\sqrt{2}$ and the growing indications for the non maximality of θ_{23} [18,19] deviate significantly from the TBM pattern, models based on TBM mixing at LO with NLO corrections coming from both the neutrino and charged lepton sectors are still viable in explaining the neutrino mixing angles. The advantage of the RS- A_4 model remain in its relative simplicity and the fact that NP

contributions to cLFV processes are very suppressed. When specializing to the brane localized case, the resulting simplifications fix θ_{13} by a single (real) parameter and the remaining two parameters are first assumed to be equal up to a phase to look for possible correlations among the predictions. Indeed, we find a very strong correlation between the value of θ_{13} (close to 9°) and the deviation from maximality of θ_{23} towards the first (second) octant for the “positive” (“negative”) cases, as can be seen in Fig. 5. In the same context it is worth mentioning a slightly different approach [34,41], in which the parameter space of the model is narrowed down to include only the VEVs of four flavons ($\underline{\mathbf{3}}, \underline{\mathbf{1}}, \underline{\mathbf{1}}', \underline{\mathbf{1}}''$), corresponding to four input parameters in the $Z_{2,3}$ preserving cases. These parameters are thus over-constrained by the existing neutrino measurements and the existence of a non trivial solution to this system of constraints reflects the suitability of A_4 as a flavor symmetry for the lepton sector. Another interesting example is the so called “special” A_4 models described in [31], where one is able to obtain a significantly better success rate $\xi_{A_4}^{spc.} \simeq 50\%$. An example for such a model can be found in [42].

Turning back to the charged lepton sector, we have studied in detail the way in which KK mixing effects of gauge bosons and fermions generate flavor violating Z couplings in charge of tree level FCNC. Due to the form diagonalizability of the LO mass matrices, the anomalous Z couplings are generated at the NLO by “cross-brane” effects which break A_4 completely. We have obtained analytical approximations to the anomalous $Z\mu e$ coupling using an effective field theory approach, in which all KK modes are integrated out. It was shown that the structure of the (non-custodian) corrections to the LH and RH Z coupling matrices (Eqs. (43) and (49)) are governed by the RH diagonalization matrices, implying a further suppression of $f_\chi^\mu(m_e/m_\mu)$ compared to the anarchic case and thus a partial protection against tree level FCNC. The results of the exact numerical diagonalization are in excellent agreement with the analytical approximations and are depicted in the left plot Fig. 7. We realize that the current upper bounds from SINDRUM II [21] eliminates roughly 35% of the model points for $\Lambda_{IR} \simeq 1.5$ TeV, implied by EWPM. As for future Muon decay and conversion experiments, it can be seen that a non observation of $\mu \rightarrow e$ conversion in DeeMEE [22] ($\text{Br}(\mu \rightarrow e) \lesssim \mathcal{O}(10^{-14})$) already eliminates roughly 93% of the model points. To release this constraint we have to reduce the strength of cross brane interactions in the charged lepton sector, which forces us to re-match the neutrino mixing angles by gradually pushing the 5D Yukawas in the neutrino sector closer to their perturbativity limit ($|Y| \lesssim 10$). A continued non observation of $\mu \rightarrow e$ in MU2e [26], COMET [23], PRIME [24] and Project-X [27] will require very weak charged lepton “cross-brane” interactions and thus a too large value for Y . Turning off the “cross-talk” between the UV and IR brane, implies a complete protection from both gauge and fermionic KK mixing effects, as is the case for the earlier brane localized versions of RS- A_4 [5,6]. The latter protection stems from the fact that at LO no RH rotation is necessary ($V_R^\ell = \mathbb{1}$) and thus one can always find a basis in which the kinetic and mass terms are simultaneously diagonal, which completely forbids tree level FCNC. These conclusions also hold true once we consider the full KK mass matrix since all 3×3 blocks mimic the structure of the ZMA mass matrices. In particular, the blocks corresponding to interactions with the custodians ($\tilde{e}_{L,R}^{(1+-)}, \tilde{\mu}_{L,R}^{(1+-)}, \tilde{\tau}_{L,R}^{(1+-)}$) have the same structure as the Dirac mass matrix

(Eq. (13)), which in turn is also diagonalized by the same rotation $V_{L,R}^{\nu D} = V_L^\ell = U(\omega)$. Thus, the RS- A_4 setup is interesting for cLFV, due to the non-custodial protection mechanism of the Z coupling matrices by virtue of the leading order “form diagonalizability”, which survives to a certain extent when cross-brane interactions are turned on.

To summarize, we wish to stress that while anarchy is still viable in explaining the neutrino mixing pattern, we have chosen here the approach of looking for an underlying structure that can account for non trivial correlations among observables. It remains to be seen what future experimental data will tell us. Moreover, anarchic models generally imply a larger amount of flavor violation and are thus subject to stronger indirect constraints. Rather inevitably, the most common protection mechanisms developed to relax these constraints, need again to invoke a certain degree of underlying flavor symmetries.

References

- [1] A. Kadosh and E. Pallante, “An A_4 flavor model for quarks and leptons in warped geometry,” *JHEP* **08** (2010) 115, 1004.0321.
- [2] E. Ma and G. Rajasekaran, “Softly broken $A(4)$ symmetry for nearly degenerate neutrino masses,” *Phys.Rev.* **D64** (2001) 113012, hep-ph/0106291.
- [3] G. Altarelli and F. Feruglio, “Tri-bimaximal neutrino mixing, $A(4)$ and the modular symmetry,” *Nucl.Phys.* **B741** (2006) 215–235, hep-ph/0512103.
- [4] L. Randall and R. Sundrum, “A large mass hierarchy from a small extra dimension,” *Phys. Rev. Lett.* **83** (1999) 3370–3373, hep-ph/9905221.
- [5] C. Csaki, C. Delaunay, C. Grojean, and Y. Grossman, “A Model of Lepton Masses from a Warped Extra Dimension,” *JHEP* **0810** (2008) 055, 0806.0356.
- [6] F. del Aguila, A. Carmona, and J. Santiago, “Neutrino Masses from an A_4 Symmetry in Holographic Composite Higgs Models,” *JHEP* **1008** (2010) 127, 1001.5151.
- [7] X.-G. He, Y.-Y. Keum, and R. R. Volkas, “ $A(4)$ flavor symmetry breaking scheme for understanding quark and neutrino mixing angles,” *JHEP* **0604** (2006) 039, hep-ph/0601001.
- [8] K. Agashe, A. Delgado, M. J. May, and R. Sundrum, “RS1, custodial isospin and precision tests,” *JHEP* **0308** (2003) 050, hep-ph/0308036.
- [9] M. S. Carena, E. Ponton, J. Santiago, and C. Wagner, “Electroweak constraints on warped models with custodial symmetry,” *Phys.Rev.* **D76** (2007) 035006, hep-ph/0701055.
- [10] A. Kadosh and E. Pallante, “CP violation and FCNC in a warped A_4 flavor model,” *JHEP* **1106** (2011) 121, 1101.5420.

- [11] K. Agashe, G. Perez, and A. Soni, “Flavor structure of warped extra dimension models,” *Phys.Rev.* **D71** (2005) 016002, hep-ph/0408134.
- [12] O. Gedalia, G. Isidori, and G. Perez, “Combining Direct & Indirect Kaon CP Violation to Constrain the Warped KK Scale,” *Phys.Lett.* **B682** (2009) 200–206, 0905.3264.
- [13] **RENO collaboration** Collaboration, J. Ahn *et. al.*, “Observation of Reactor Electron Antineutrino Disappearance in the RENO Experiment,” *Phys.Rev.Lett.* **108** (2012) 191802, 1204.0626.
- [14] **DAYA-BAY Collaboration** Collaboration, F. An *et. al.*, “Observation of electron-antineutrino disappearance at Daya Bay,” *Phys.Rev.Lett.* **108** (2012) 171803, 1203.1669.
- [15] **DOUBLE-CHOOZ Collaboration** Collaboration, Y. Abe *et. al.*, “Indication for the disappearance of reactor electron antineutrinos in the Double Chooz experiment,” *Phys.Rev.Lett.* **108** (2012) 131801, 1112.6353.
- [16] **T2K Collaboration** Collaboration, K. Abe *et. al.*, “Indication of Electron Neutrino Appearance from an Accelerator-produced Off-axis Muon Neutrino Beam,” *Phys.Rev.Lett.* **107** (2011) 041801, 1106.2822.
- [17] **MINOS Collaboration** Collaboration, P. Adamson *et. al.*, “Improved search for muon-neutrino to electron-neutrino oscillations in MINOS,” *Phys.Rev.Lett.* **107** (2011) 181802, 1108.0015.
- [18] G. Fogli, E. Lisi, A. Marrone, D. Montanino, A. Palazzo, *et. al.*, “Global analysis of neutrino masses, mixings and phases: entering the era of leptonic CP violation searches,” *Phys.Rev.* **D86** (2012) 013012, 1205.5254.
- [19] D. Forero, M. Tortola, and J. Valle, “Global status of neutrino oscillation parameters after Neutrino-2012,” *Phys.Rev.* **D86** (2012) 073012, 1205.4018.
- [20] **SINDRUM Collaboration** Collaboration, U. Bellgardt *et. al.*, “Search for the Decay $\mu^+ \rightarrow e^+ e^+ e^-$,” *Nucl.Phys.* **B299** (1988) 1.
- [21] **SINDRUM II Collaboration** Collaboration, P. Wintz *et. al.*, “Test of LFC in $\mu \rightarrow e$ conversion on titanium,”.
- [22] The DEEMEE collaboration, “A proposal for a muon-electron conversion experiment in J-PARC,” <http://deeme.hep.sci.osaka-u.ac.jp/> (2012).
- [23] Kuno, Y. for the COMET collaboration, “Experimental Proposal for Phase-I of the COMET Experiment at J-PARC,” http://j-parc.jp/researcher/Hadron/en/pac_1207/pdf/E21_2012-10.pdf (2013).

- [24] Aoki, M. et al. for the PRIME/PRISM collaboration, “Experimental Proposal for Phase-I of the COMET Experiment at J-PARC,” http://j-parc.jp/researcher/Hadron/en/pac_0606/pdf/p20-Kuno.pdf (2013).
- [25] Kuno, Y. for the MuSIC collaboration, “A proposal for a muon-electron conversion experiment in RCNP Osaka,” http://nufact09.iit.edu/wg4/wg4_yoshida-music.pdf.
- [26] The Mu2e collaboration, “A proposal for a muon-electron conversion experiment in Fermilab,” <http://mu2e.fnal.gov/public/index.shtml> (2012).
- [27] Mu2e collaboration, “A proposal for a muon-electron conversion experiment in the Project X proton accelerator at Fermilab,” <http://projectx.fnal.gov/> (2012).
- [28] Mu3e collaboration, “A Search for the forbidden decay $\mu \rightarrow e^+e^+e^-$,” <http://www.psi.ch/mu3e/> (2012).
- [29] P. Harrison, D. Perkins, and W. Scott, “Tri-bimaximal mixing and the neutrino oscillation data,” *Phys.Lett.* **B530** (2002) 167, [hep-ph/0202074](#).
- [30] W. D. Goldberger and M. B. Wise, “Modulus stabilization with bulk fields,” *Phys.Rev.Lett.* **83** (1999) 4922–4925, [hep-ph/9907447](#).
- [31] G. Altarelli, F. Feruglio, L. Merlo, and E. Stamou, “Discrete Flavour Groups, θ_{13} and Lepton Flavour Violation,” *JHEP* **1208** (2012) 021, [1205.4670](#).
- [32] M. Hirsch, D. Meloni, S. Morisi, S. Pastor, E. Peinado, *et. al.*, “Proceedings of the first workshop on Flavor Symmetries and consequences in Accelerators and Cosmology (FLASY2011),” [1201.5525](#).
- [33] I. de Medeiros Varzielas, C. Hambroek, G. Hiller, M. Jung, P. Leser, *et. al.*, “Proceedings of the 2nd Workshop on Flavor Symmetries and Consequences in Accelerators and Cosmology (FLASY12),” [1210.6239](#).
- [34] M.-C. Chen, J. Huang, J.-M. O’Bryan, A. M. Wijangco, and F. Yu, “Compatibility of θ_{13} and the Type I Seesaw Model with A_4 Symmetry,” *JHEP* **1302** (2013) 021, [1210.6982](#).
- [35] C. Csaki, J. Erlich, and J. Terning, “The Effective Lagrangian in the Randall-Sundrum model and electroweak physics,” *Phys.Rev.* **D66** (2002) 064021, [hep-ph/0203034](#).
- [36] A. J. Buras, B. Duling, and S. Gori, “The Impact of Kaluza-Klein Fermions on Standard Model Fermion Couplings in a RS Model with Custodial Protection,” *JHEP* **0909** (2009) 076, [0905.2318](#).
- [37] W.-F. Chang and J. N. Ng, “Lepton flavor violation in extra dimension models,” *Phys.Rev.* **D71** (2005) 053003, [hep-ph/0501161](#).

- [38] G. Feinberg, P. Kabir, and S. Weinberg, “Transformation of muons into electrons,” *Phys.Rev.Lett.* **3** (1959) 527–530.
- [39] **MEG Collaboration** Collaboration, J. Adam *et. al.*, “New constraint on the existence of the $\mu^+ \rightarrow e^+\gamma$ decay,” 1303.0754.
- [40] G. Altarelli, F. Feruglio, I. Masina, and L. Merlo, “Repressing Anarchy in Neutrino Mass Textures,” *JHEP* **1211** (2012) 139, 1207.0587.
- [41] H. Ishimori and E. Ma, “New Simple A_4 Neutrino Model for Nonzero θ_{13} and Large δ_{CP} ,” *Phys.Rev.* **D86** (2012) 045030, 1205.0075.
- [42] Y. Lin, “Tri-bimaximal Neutrino Mixing from $A(4)$ and $\theta(13) \sim \theta(C)$,” *Nucl.Phys.* **B824** (2010) 95–110, 0905.3534.